Cell Death and Differentiation (2005) 12, 734–750

www.nature.com/cdd

Impaired homeostasis and phenotypic abnormalities in *Prdx6*$^{-/-}$ mice lens epithelial cells by reactive oxygen species: increased expression and activation of TGFβ

N Fatma[1], E Kubo[2], P Sharma[1], DR Beier[3] and DP Singh*[,1]

[1] Department of Ophthalmology, University of Nebraska Medical Center, Omaha, NE 68198, USA
[2] Department of Ophthalmology, University of Fukui, Fukui, Japan
[3] Division of Genetics, Brigham and Women's Hospital, Harvard Medical School, Boston, MA, USA
* Corresponding author: DP Singh, Department Ophthalmology, University of Nebraska Medical Center, 985540 Nebraska Medical Center, Omaha, NE 68198-5840, USA. Tel: +1 402 559 8805; Fax: +1 402 559 8808; E-mail: dpsingh@unmc.edu.

Received 20.8.04; revised 28.12.04; accepted 14.1.05; published online 01.4.05
Edited by S Roy

Abstract

PRDX6, a member of the peroxiredoxins (PRDXs) family, is a key player in the removal of reactive oxygen species (ROS). Using targeted inactivation of the *Prdx6* gene, we present evidence that the corresponding protein offsets the deleterious effects of ROS on lens epithelial cells (LECs) and regulates gene expression by limiting its levels. PRDX6-depleted LECs displayed phenotypic alterations and elevated α-smooth muscle actin and βig-h3 expression (markers for cataractogenesis), indistinguishable from transforming growth factor β (TGFβ)-induced changes. Biochemical assays disclosed enhanced levels of ROS, as well as high expression and activation of TGFβ1 in *Prdx6*$^{-/-}$ LECs. A CAT assay revealed transcriptional repression of lens epithelium-derived growth factor (LEDGF), HSP27, and αB-crystallin promoter activities in these cells. A gel mobility shift assay demonstrated the attenuation of LEDGF binding to heat shock or stress response elements present in these genes. A supply of PRDX6 to *Prdx6*$^{-/-}$ LECs reversed these changes. Based on the above data, we propose a rheostat role for PRDX6 in regulating gene expression by controlling the ROS level to maintain cellular homeostasis.

Cell Death and Differentiation (2005) **12,** 734–750.
doi:10.1038/sj.cdd.4401597
Published online 1 April 2005

Keywords: reactive oxygen species; phenotypic changes; TGFβ; LEDGF; apoptosis; oxidative stress; PRDX6; AOP2

Abbreviations: AOP2, antioxidant protein 2; LEDGF, lens epithelium-derived growth factor; PRDX, peroxiredoxin; ROS, reactive oxygen species; SDS-PAGE, sodium dodecyl sulfate polyacrylamide gel electrophoresis; TGFβ, transforming growth factor β; TIE, transforming growth factor β inhibitory element

Introduction

Reactive oxygen species (ROS) and organic free radicals are essential metabolic intermediates with important regulatory functions. Overproduction of these reactive metabolites or ROS is implicated in the etiology of a host of degenerative diseases,[1] including age-related cataractogenesis. Of the various types of oxidative damage, apoptosis, loss of homeostasis, and abnormal phenotypic changes are major contributors to injury. Thus, strict regulation of ROS is vital to maintain cellular integrity and homeostasis. Antioxidants play a major role in this regard by limiting the overproduction of radicals generated by the metabolism or cells under environmental stress. The major defense enzymes reported to date are superoxide dismutase (SOD), which converts superoxide radicals to hydrogen peroxide (H_2O_2), catalase (CAT), selenium (SE)-dependent glutathione peroxidase (GSHPx), glutathione-*S*-transferase (GST), and the recently defined rapidly growing family of peroxiredoxins (PRDXs)[2,3]. These enzymes reduce peroxides to the corresponding alcohol or water.[4–8] The PRDX family displays special features, compared with other existing peroxidases. Specifically, when reducing H_2O_2, PRDX enzymes themselves are oxidized, therefore acting both as peroxidase and co-substrate.[9] Recent studies have shown that the active site cysteine of PRDXs is selectively oxidized to cysteine sulfinic acid, leading to inactivation of peroxidase activity, and the sulfinic form of PRDX is rapidly reduced to the catalytically active thiol form.[10,11] It appears that the cell's ability to reduce protein sulfinic acid serves as a mechanism to repair damaged proteins or represents a new type of cyclic modification regulating the functions of various proteins.

PRDXs, thiol-containing peroxidases, are conserved from bacteria to mammals.[10,12] There are six subgroups of PRDX enzymes (PRDX1–6) in mammals.[12–14] These enzymes use redox-active cysteines to reduce peroxides, and are divided into two categories, 1-Cys and 2-Cys, based on the number of cysteinyl residues directly involved in catalysis[3]. The peroxidase reaction is composed of two steps centered around a redox-active cysteine designated 'peroxidatic cysteine'.[15,16] The 1-Cys PRDX contains only the peroxidatic cysteine, and not a resolving cysteine.[16] Based on the presence of one conserved redox-active cysteine in the NH2 terminus of PRDX6 (C-47), previously known as antioxidant protein 2 (AOP2)[2,3,17–20] in contrast to two conserved cysteine residues in the rest of the PRDX family, the Mouse Genomic Nomenclature Committee (MGNC) and Human Gene Nomenclature Committee (HGNC) put this molecule under subgroup 6, now known as PRDX6.[12]

H_2O_2, a source of oxidative stress, has gained attention recently due to its role as a cellular signaling factor for various cytokines and growth factors, including platelet-derived growth factor (PDGF), insulin-like growth factor (IGF),

endothelial-derived growth factor (EGF), tumor necrosis factor α (TNF-α), and transforming growth factor β (TGFβ). The generation of ROS by these molecules is associated with the activation or deactivation and modulation of expression of several anti-death transcription factors, including lens epithelium-derived growth factor (LEDGF).[21,22] LEDGF is a survival factor that acts as a transcriptional factor[17,23–25] by activating heat shock element (HSE; nGAAn) and a stress-related element (STRE; T/AGGGGA/T).[17,25,26] Cells overexpressing LEDGF contain elevated levels of PRDX6 protein and mRNA, and survive longer under oxidative and heat stress conditions.[17]

Moreover, earlier studies have demonstrated that TGFβ plays a regulatory role in gene transcription, and some genes comprise TGFβ inhibitory elements (TIE).[27,28] Our experiments establish the presence of TIE in the LEDGF promoter.[29] TGFβ inhibits the gene transcription of LEDGF.[29] TGFβ is present in ocular media, and various levels of activity have been reported in the aqueous and vitreous forms in human and other species.[30–33] Interestingly, an increased level of H_2O_2 in aqueous media is reported.[34] However, further investigation is required to understand the diverse biological effects of TGFβ and ROS in the eye lens system. TGFβ increases the ROS intracellular content in different cell types, and some of its action may be mediated by oxidative stress. Recent reports have demonstrated that TGFβ increases ROS by rapid downregulation of antioxidant genes.[35–38] Evidence shows that overexpression of PRDX6 reduces ROS generated in response to growth factors.[39,40] To determine the potential role of PRDX6 in reducing oxidative stress and acting as an antioxidant defense *in vitro* and *in vivo,* we utilized *Prdx6* knockout mice. Cells derived from *Prdx6* knockout mice were more susceptible to cellular damage, and showed phenotypic changes. Our findings are in agreement with several reports demonstrating the activation of TGFβ as a result of ROS elevation. [31,32,41,42] The most striking morphological differences between *Prdx6*$^{+/+}$ cells and *Prdx6*$^{-/-}$ cells are accounted for by expression pattern changes due to a single gene, *Prdx6.* The physiological consequences of *Prdx6* knockout are notable. LEDGF and associated genes are suppressed, indicating that changes in lens epithelial cells (LECs) may be associated to dysfunction of LEDGF.

In the present study, we examine the effects of PRDX6 on LECs survival and integrity under stress and nonstress environmental conditions. We additionally determine whether PRDX6-depleted cells are more susceptible to oxidative stress and modulate expression and function of LEDGF or its stress-associated genes, and analyze their functional association with TGFβ. PRDX6-depleted cells displayed diminished DNA-binding activity of LEDGF and its regulated genes. Using *Prdx6*$^{-/-}$ LECs, we demonstrate that PRDX6 protects cells by limiting the ROS level, and plays a regulatory role in gene transcription. In addition, our results provide novel information on ROS activation, expression of TGFβ1 and its effects on gene modulation, such as repression of LEDGF transcription and stress-associated genes in LECs, which in turn may disrupt cellular integrity, thereby contributing to our understanding of the pathophysiology of plausible age-associated degenerative diseases, including cataractogenesis. PRDX6 abolishes ROS-mediated deleterious effects in LECs, and may therefore have significant potential to postpone age-associated degenerative disorders.

Results

PRDX6 is highly expressed in murine ocular lenses, and *Prdx6*$^{-/-}$ mice lenses display higher susceptibility to oxidative stress and abnormal migration of LECs

We reported earlier that PRDX6 is present in ocular lens and removes intra- and extracellular H_2O_2.[17] According to a recent classification, the PRDX family is comprised of six members (PRDX1–6). We initially examined all the members of the PRDX family in mice lens. PRDX5 and PRDX6 were expressed significantly. Real-time PCR data revealed higher levels of PRDX6 (Figure 1A). This finding indicates that the expression of PRDXs may be tissue- or organ-specific. The function of PRDX6 appears pivotal, at least in lens, because other PRDXs could not inhibit the changes of *Prdx6*$^{-/-}$ LECs. To evaluate the potential roles of PRDX6 in reducing oxidative stress, acting as antioxidant defense, and in signaling, we used *Prdx6* knockout mice. Interestingly, lenses from PRDX6-depleted mice exhibited significant susceptibility to oxidative stress and opacity in the superficial cortex following exposure to H_2O_2 (200 μM) for 44 h (Figure 1B). In addition, the histological sections of lenses isolated from *Prdx6*$^{-/-}$ mice revealed abnormal cellular localization in the bow region and thickening of capsule. Moreover, some epithelial cells migrated to the region posterior to the equator (Figure 1C, left panel). These findings signify the physiological importance of PRDX6 in lens. Since it is difficult to determine all the biochemical and molecular biological parameters in whole lenses, we generated *Prdx6*$^{-/-}$ LEC lines to specifically identify the roles of PRDX6. Notably, lenses/LECs isolated from *Prdx6*$^{+/+}$ (heterozygous) mice were indistinguishable from those of wild-type animals. PRDX6 protein expression was comparable in lenses/LECs of both groups and a similar finding has been reported by other groups.[43] Accordingly, we utilized wild-type mice and homozygous lenses/LECs throughout the study.

Generation and validation of LECs isolated from the lenses of *Prdx6*$^{-/-}$ and *Prdx6*$^{+/+}$ mice

We generated a LEC line from lenses isolated from Prdx6-targeted mutants *(Prdx6*$^{-/-}$) and wild-type (*Prdx6*$^{+/+}$) mice. Western analysis and RT-PCR using PRDX6-specific antibody[17] and primers, respectively, revealed an absence of PRDX6 mRNA and protein in LECs from homozygous mutants, in contrast to wild type (Figure 1D and E). Next, we validated whether cells isolated from the lenses are indeed LECs. Western analysis using the αA-crystallin antibody confirmed the presence of αA-crystallin, a specific marker of LECs, in both *Prdx6*$^{-/-}$ and *Prdx6*$^{+/+}$ LECs (Figure 1F).

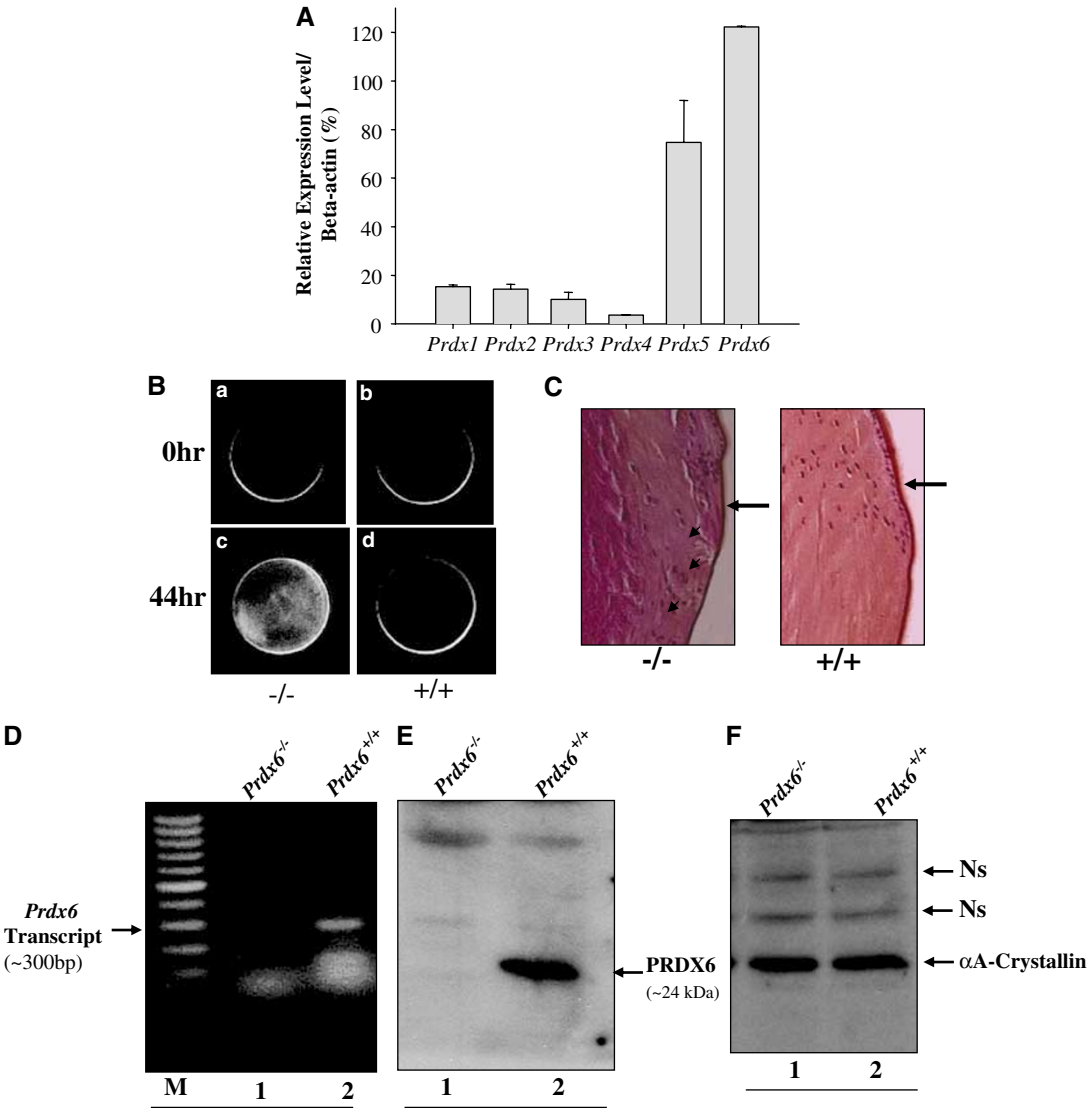

Figure 1 (**A**) Quantitative real-time PCR showing differential expression of *PRDX1*–6 mRNA in normal mouse lens. Total RNA from mouse lenses (12-week-old) was isolated and transcribed into cDNA. Real-time PCR was carried out using specific primers.[43] mRNA expression of each PRDX was adjusted to the mRNA copies of β-actin. Results indicated that mRNA expression level of PRDX6 was significantly high in comparison to other PRDXs. However, PRDX5 is also present at a significant level but could not control cellular integrity of LEC. Thus PRDX6 has pivotal role in maintaining the normal physiological function of LECs. (**B**, **C**) Lenses from *Prdx6*$^{-/-}$ mouse are more susceptible to oxidative stress and reveal abnormal histology. Lenses from 8-month-old *Prdx6*$^{-/-}$ and *Prdx6*$^{+/+}$ mice were subjected to oxidative stress (see Materials and Methods) and photomicrographed. Opacity could be observed in lenses isolated from *Prdx6*$^{-/-}$ (**Ic**, left panel) compared to *Prdx6*$^{+/+}$ (**1d**, right panel). Histological analysis of PRDX6-depleted lens showed abnormal migration of LECs; LECs from bow region migrated to posterior subcapsular space and anucleation was impaired (a process of terminal differentiation). Large arrows indicate bow region and arrowheads indicate LECs that have migrated to the posterior region. These data support the concept that PRDX6 has intrinsic biological activity and play a pivotal role in maintaining lens homeostasis. (**D**–**F**) Validation of *Prdx6*$^{-/-}$ and *Prdx6*$^{+/+}$ LECs using RT-PCR and Western analysis showing the absence and presence of PRDX6 transcript (**D**) and protein (**E**). mRNA was isolated from the cultured cells and subjected to RT-PCR with primers specific to *Prdx6*. Resulting products were visualized on agarose gel with EtBr staining. 'M' represents 100 bp DNA marker. Western analysis showing the presence of PRDX6 protein in *Prdx6*$^{+/+}$ cells (**E**). Cell lysate was prepared using RIPA buffer and used for protein blotting with anti-PRDX6 antibody and visualized. Western blot showing the expression of αA-crystallin in *Prdx6*$^{-/-}$ and *Prdx6*$^{+/+}$ cells (**F**). Ns denotes equal loading of samples. The extracted protein was blotted and immunostained with anti-αA-crystallin antibody

Phenotypic changes in *Prdx6*$^{-/-}$ LECs resemble TGFβ-induced changes in LECs

We harvested *Prdx6*$^{-/-}$ and *Prdx6*$^{+/+}$ LECs, either with complete media or DMEM containing 0.1% BSA. Cells were analyzed at variable time intervals (24, 48, 72, and 96 h) and photomicrographed. Surprisingly, significant phenotypic alterations were observed in PRDX6-depleted LECs expressing α-smooth muscle actin (α-SM actin), a biological marker for cataractogenesis (Figure 2B, a). Careful microscopic observation revealed that cells became elongated and fiber-like, formed cellular aggregates, and packed irregularly. Moreover, these cells detached more frequently, and

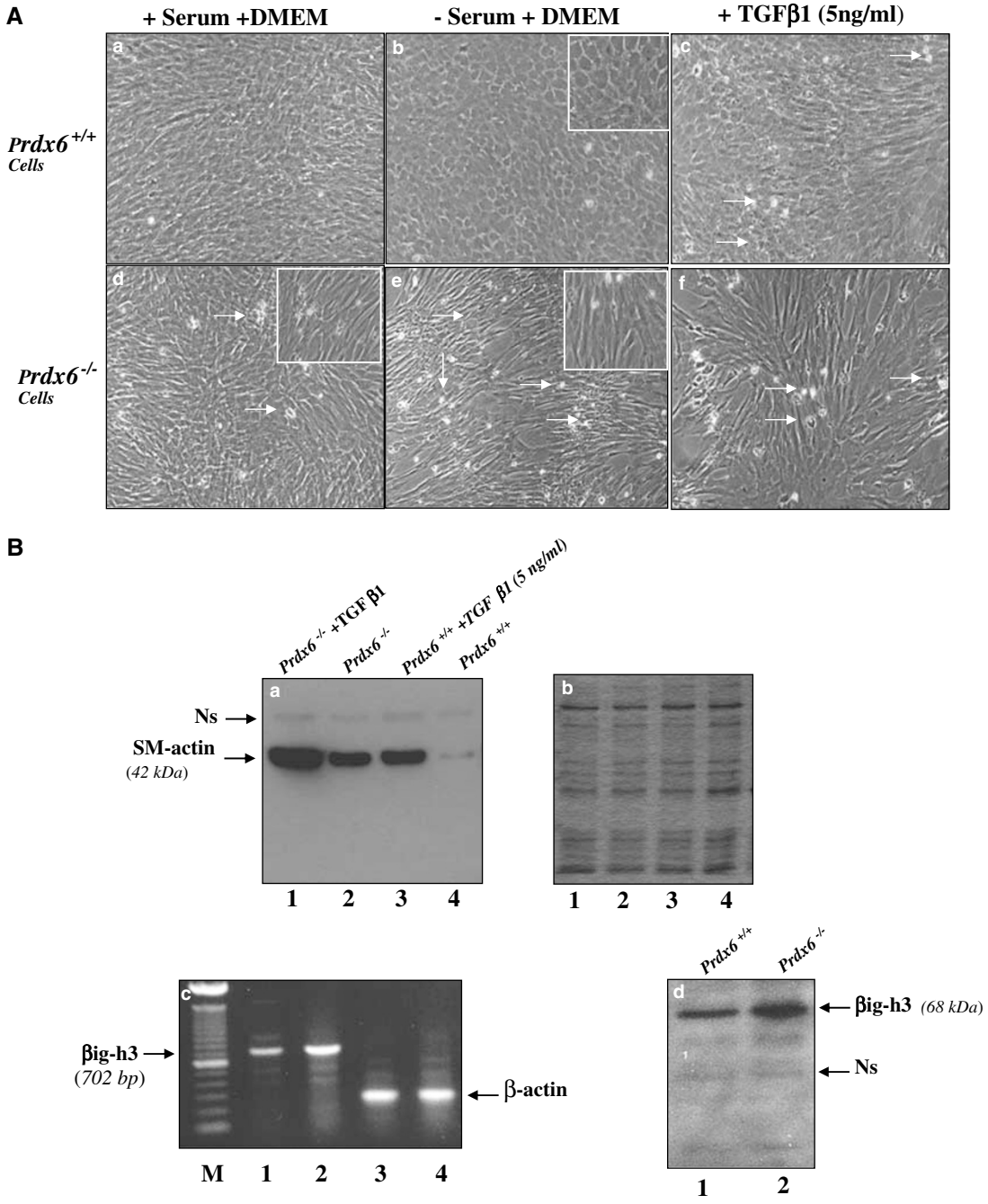

Figure 2 (**A**) *Prdx6*$^{-/-}$ cells showing phenotypic changes in cell culture that resemble TGFβ-induced changes of LECs. *Prdx6*$^{+/+}$ and *Prdx6*$^{-/-}$ cells were cultured in DMEM either with complete medium (**a** and **d**) or with 0.1% BSA (**b** and **e**). Under serum depletion condition, cells became elongated and fiber-like, formed cellular aggregates, packed irregularly and showed cellular death (**e**) and this effect was more prominent if TGFβ was added to these cells (**f**). When *Prdx6*$^{+/+}$ LECs were exposed to TGFβ at 5 ng/ml, changes in cellular morphology were similar to the changes observed in PRDX6-depleted cells (**c**). (**B**) Western analysis showing expression of α-SM actin and βig-h3 in *Prdx6*$^{-/-}$ cells. A band of 42 kDa could be seen following immunostaining with anti-α SM actin-specific antibody in *Prdx6*$^{-/-}$ cells (**a**). *Prdx6*$^{+/+}$ cells did not express α-SM actin (**a**, lane 4) but expressed when treated with TGFβ (**a**, lane 3) and **b**; corresponding Commassie-stained gel showing equal loading of protein samples. *Prdx6*$^{-/-}$ LECs showed increased expression of βig-h3 protein (**d**, lane 2) and transcript (**c**, lane 2)

underwent spontaneous death, leading to increased intracellular spaces. A photomicrograph taken after 96 h is presented (Figure 2A, e). Interestingly, these differences were evident in cells cultured with complete media, but not as distinguishable as in those cultured under serum depletion conditions (Figure 2A, d). This may be due to the presence of catalase in serum. Notably, lenses were isolated from systematic blood circulation. Thus, the morphological integrity of LECs without serum reflects the *bona fide* phenotype of LECs *in vivo.* To further determine whether TGFβ-inducible gene (*βig-h3*) is

expressed in *Prdx6*$^{-/-}$ cells, Western blots were conducted using anti-βig-h3 antibody. Elevated levels of this protein were observed in *Prdx6*$^{-/-}$ cells (Figure 2B, d, lane 2), suggesting a TGFβ-mediated effect. In view of our previous report[29] and data from other laboratories,[44–46] we hypothesize that phenotypic changes and expression of α-sm actin in PRDX6-depleted LECs are associated with TGFβ. Initially, we verified the presence of TGFβ RI[29] and RII[47] receptors in *Prdx6*$^{-/-}$ LECs by Western analysis (data not shown). Next, we exposed *Prdx6*$^{+/+}$ LECs to different concentrations of TGFβ for variable time intervals. Changes in cellular morphology were analyzed and photomicrographed, and compared to a parallel culture of *Prdx6*$^{-/-}$ LECs. Interestingly, TGFβ-induced changes in LECs were similar to those of PRDX6-depleted LECs (Figure 2A, c). These cells additionally express α-SM actin (Figure 2B, a). From these results, we conclude that phenotypic changes as well as expression of α-SM actin and βig-h3 in *Prdx6*$^{-/-}$ cells are associated with TGFβ activation.

Prdx6$^{-/-}$ cells are highly susceptible to oxidative stress and undergo apoptosis

To determine the functional significance of PRDX6 inactivation, we assessed the cellular survival of LECs after oxidative stress. PRDX6 removes H_2O_2 and protects cells. Therefore, PRDX6-depleted cells should be highly susceptible to oxidative stress. To this end, LECs were subjected to oxidative stress using H_2O_2 for 2 h. As expected, PRDX6-depleted cells were more vulnerable to oxidation-induced cell death (Figure 3A, b and B). Next, we performed DAPI staining (data not shown) and a TUNEL assay. Cells were photomicrographed and analyzed. Typical apoptic nuclei (fragmented and disintegrated) were observed in PRDX6-depleted cells (Figure 3A, d). It is thus evident from the data that PRDX6-depleted cells undergo apoptosis during oxidative stress. In contrast, *Prdx6*$^{+/+}$ LECs were resistant to identical oxidative stress, demonstrating an antioxidant role of PRDX6. Various reports show that higher levels of ROS are a common signal in different cell death pathways, and indicate a complex relationship between ROS levels and cell death,[48–50] in view of the finding that PRDX6-depleted cells bear higher levels of ROS, and are thereby more susceptible to oxidative stress.

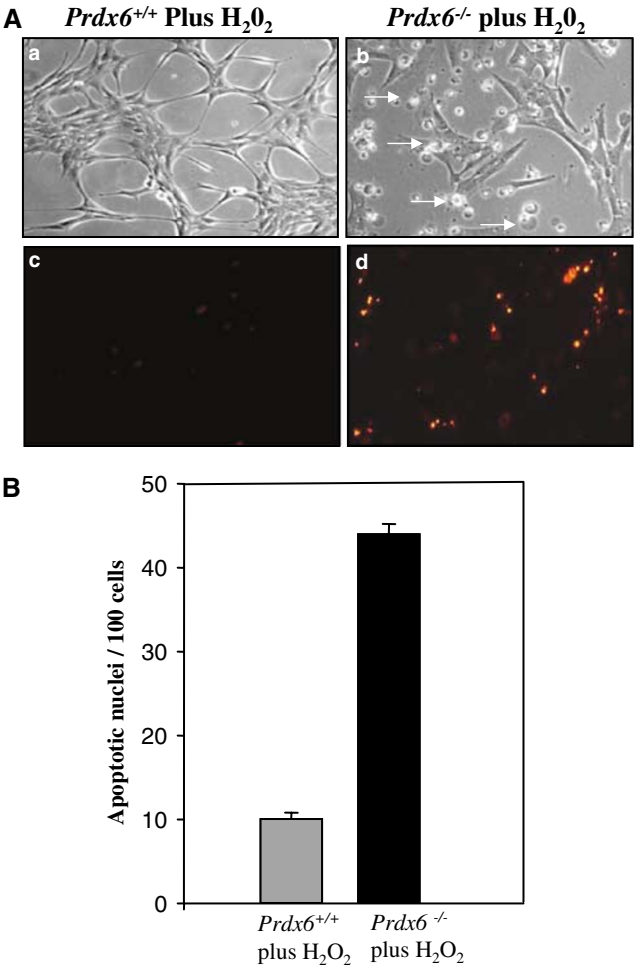

Figure 3 *Prdx6*$^{-/-}$ LECs are highly susceptible to oxidative stress. (**A**) Cells were cultured in DMEM + 10% FBS (3×10^5 cells per well in a six-well plate). On the second day, cells were exposed to 10 μM H_2O_2 for 2 h. After 24 h of recovery period, cells were photomicrographed. A significant number of cell death could be observed in *Prdx6*$^{-/-}$ cells (**A**; **b**). TUNEL assay showed more apoptotic cell death in *Prdx6*$^{-/-}$ cells (**A**; **d**). (**B**) Number of apoptotic cells/100 cells were counted and are presented in the histogram

Activation of TGFβ in PRDX6-depleted LECs is associated with ROS and inhibited by PRDX6 overexpression or MnTBAP

TGFβ induces phenotypic changes, expression of α-SM actin, and apoptosis in many cell types, including LECs. We predict that TGFβ is activated in PRDX6-depleted cells. Phenotypic changes are associated with ROS-mediated TGFβ activation. TGFβ is normally secreted in the latent form (L-TGFβ), and must be cleaved from latency-associated peptides (LAP) to produce the bioactive form.[51] ROS are implicated in the activation of latent TGFβ.[51] Quantification by staining with H2DCF-DA[42] established a higher prevalence of ROS in these cells (Figure 4A, b). However, it is noteworthy that DCF fluorescence is not specific for H_2O_2, and other oxidants such as peroxynitrite, O_2-, NO, etc. could also oxidize DCFH2 into DCF. So, DCF fluorescence reflects the overall oxidative stress in cells.[43] Next, to establish whether the expression and release of bioactive TGFβ is increased, we performed RT-PCR, Western analysis, and E_{max} ELISA Assay (Promega). The culture supernatant of *Prdx6*$^{-/-}$ LECs contained significantly higher bioactive TGFβ (Figure 5c). Additionally, these cells displayed elevated TGFβ mRNA and protein expression (Figure 5a and b). The results collectively imply that changes in LECs are associated with TGFβ. Next, we determined whether the addition of TGFβ-neutralizing antibody in culture media or overexpression with PRDX6 (GFP-PRDX6) restored the original phenotype in *Prdx6*$^{-/-}$ cells. Treatment with the TGFβ-neutralizing antibody for 72–96 h inhibited apoptosis and cell aggregation, but did not restore the original phenotype of LECs (data not shown). In contrast, *Prdx6*$^{-/-}$ LECs overexpressed with GFP-PRDX6 (*Prdx6*$^{-/-}$ LECs were transfected multiple times, and selected using

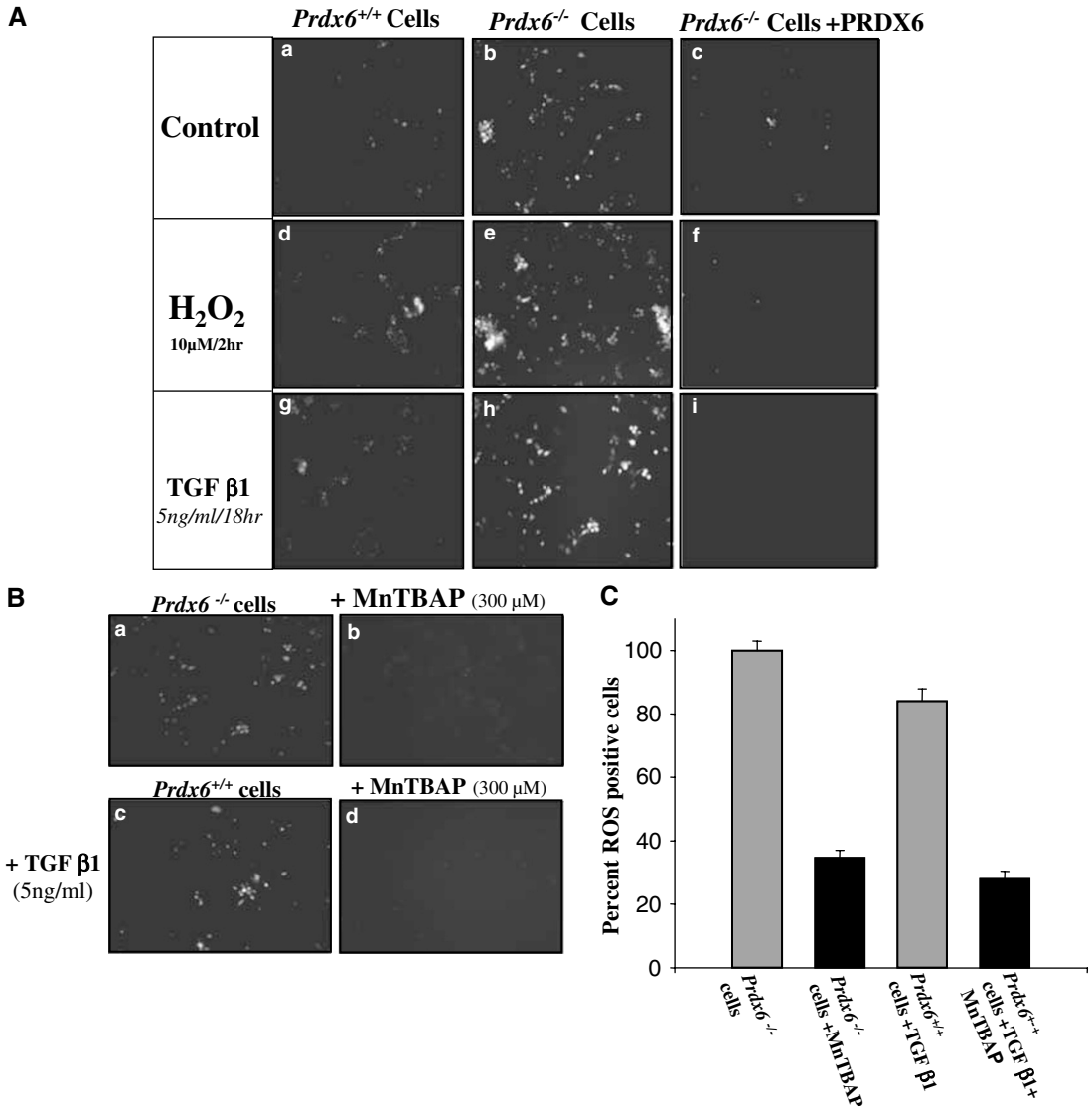

Figure 4 TGFβ treatment generates ROS in *Prdx6*$^{+/+}$ LECs. *Prdx6*$^{+/+}$ cells were exposed to TGFβ1 at 5 ng/ml and ROS level was measured. Next, *Prdx6*$^{-/-}$ (untreated) and *Prdx6*$^{+/+}$ cells treated with TGFβ1 were cultured in MnTBAP overnight at 37°C. Next day, the medium was replaced with Hank's solution containing 5 μM H_2-DCFH-DA and fluorescence intensity was measured with fluorescent microscope. Histogram represents the results (mean $\pm$ s.d. of three independent experiments each with triplicate wells) showing ROS-positive cells, and (**A**, **B**) are representatives of the experiment

Geneticin, GIBCO) revealed phenotypes identical to that of wild-type LECs. These results suggest that the changes in PRDX6-depleted LECs are not solely mediated by TGFβ, and other signals need to be additionally investigated. However, our data demonstrate the involvement of TGFβ in the damage of LECs. To further determine whether ROS are involved in cell death or TGFβ activation, we included a superoxide dismutase mimetic, MnTBAP,[42] a known ROS inhibitor. MnTBAP abrogated biologically active TGFβ in the supernatant of PRDX6-depleted cells (Figure 4B and C). Our findings establish that ROS are responsible for activation of TGFβ in PRDX6$^{-/-}$ cells.

TGFβ induces a variety of effects in a number of tissues or cells, and plays a role in the regulation of apoptosis by generating higher levels of ROS. Therefore, we envisage a vicious feedforward process in PRDX6-depleted cells. In an attempt to explain the plausible mechanism involved, we treated *Prdx6*$^{+/+}$ cells with TGFβ1, and assayed the ROS level (Figure 4A, g and C). The data support our hypothesis that ROS activates TGFβ, which in turn triggers further ROS production in cells. However, an intrinsic supply of PRDX6 or addition of MnTBAP inhibits TGFβ-induced ROS generation or changes in LECs (Figure 4A–C).

Repression of transcription of LEDGF and its associated genes, *hsp27* and *αB-crystallin*

Several reports disclose downregulation of gene expression by TGFβ-mediated signaling and show that reduced expression

is mediated at the level of transcription.[27,52–54] We determined the transcriptional potential of LEDGF, HSP27 and αB-crystallin promoters linked to CAT. LEDGF promoter constructs containing TIEs[29] (−482 to +35 (wild type; -444-gttcT**TGG**tga-433) and its mutant (mutated at -444-gttcT**ATT**tga-433) were employed to define whether repression of promoter activity is mediated by TGFβ. Our results disclose reduced promoter activity in *Prdx6*$^{-/-}$ LECs (Figure 6b), in comparison to the mutant promoter, suggesting that suppression of LEDGF is TGFβ-dependent.

Since HSP27 and αB-crystallin promoter activation depend on LEDGF binding to HSE (nGAAn) and STRE (A/TGGGGA/T) elements,[25] we analyzed whether these transcriptional activities were altered in *Prdx6*$^{-/-}$ cells. The promoter activity of αB-crystallin was decreased in *Prdx6*$^{-/-}$ LECs (Figure 7A, b), implying that the reduction in gene transcription is due to the presence of active TGFβ. Thus, it appears that by limiting ROS PRDX6 in LECs not only protects cells, but also plays a role in cell signaling.

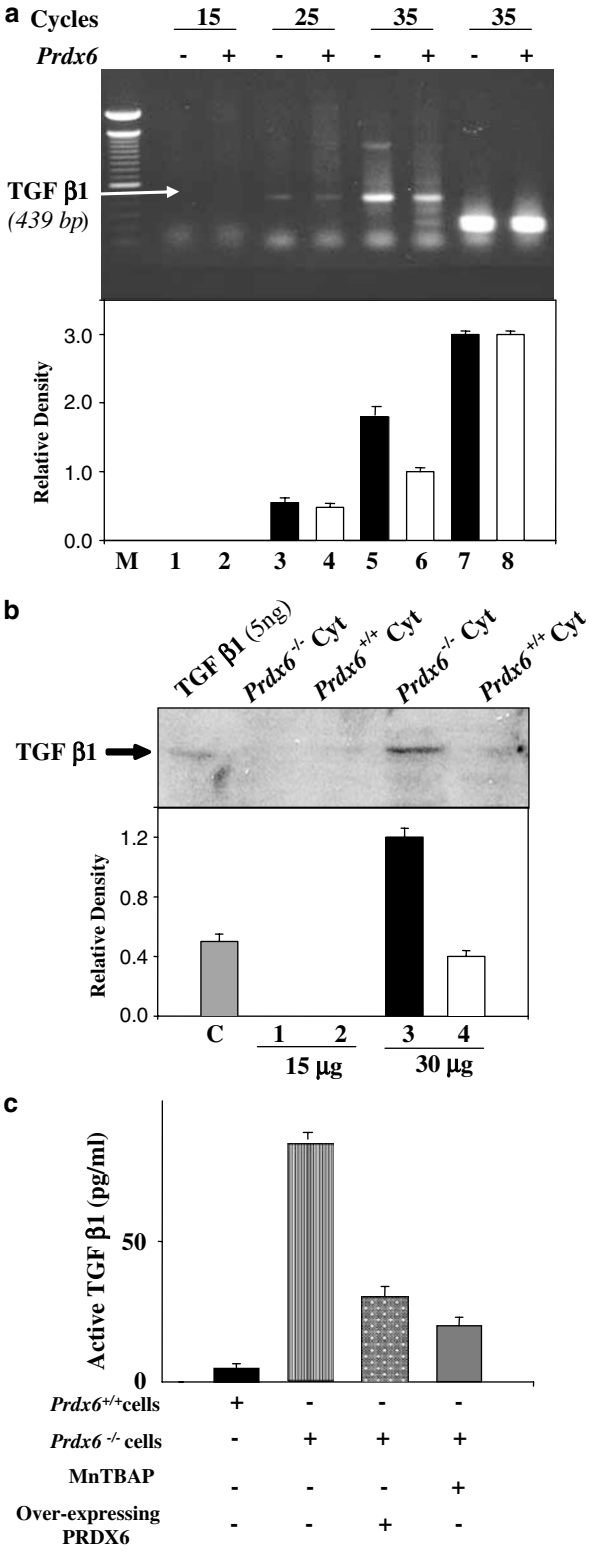

Figure 5 (**a**, **b**) RT-PCR and Western analysis showing increased levels of TGFβ1 transcript and protein in *Prdx6*$^{-/-}$ LECs. mRNA was isolated from cultured *Prdx6*$^{+/+}$ and *Prdx6*$^{-/-}$ cells, and subjected to RT-PCR with TGFβ-specific primer pair (R & D Systems, Cat no RDP-26-025) (**a**). β-Actin was used as positive control (**a**: upper panel; lanes 7 and 8); lower panel, histogram showing the relative density of TGFβ1 mRNA level. Results showed that a 439 bp TGFβ1 band was present at higher intensity in *Prdx6*$^{-/-}$ cells (**a**; lane 5) in comparison to *Prdx6*$^{+/+}$ cells (**a**; lane 6). From another set of cells, cytoplasmic extract was prepared and used for Western analysis (**b**, upper panel). The level of TGFβ protein was comparatively higher in *Prdx6*$^{-/-}$ cells (**b**; lane 3) than in *Prdx6*$^{+/+}$ cells. Lower panel, shows the relative density of protein bands. (**c**) *Prdx6*$^{-/-}$ cells secrete bioactive TGFβ1. Cells (2×10^5 cells per well) were cultured in 96-well plates for 24 h. Culture supernatant was collected and bioactive TGFβ1 was determined directly by the TGFβ1 Emax ImmunoAssay system (Promega). *Prdx6*$^{-/-}$ cells, overexpressing PRDX6 or treated with MnTBAP, were also used. A higher level of bioactive TGFβ1 was detected in *Prdx6*$^{-/-}$ cells (stripped) in comparison to *Prdx6*$^{+/+}$ cells (black bar). *Prdx6*$^{-/-}$ cells overexpressing PRDX6 showed a significant decreased in the level of bioactive TGFβ1 (dotted bar). MnTBAP, an ROS inhibitor, significantly abrogated the biologically active TGFβ (gray bar)

Supply of PRDX6 restores LEDGF, HSP27, and αB-crystallin transcription

It is evident from the above results that changes in *Prdx*$^{-/-}$ LECs are associated with ROS-mediated TGFβ activation. As PRDX6 protects cells by limiting ROS, we investigated whether the addition of PRDX6 affected the promoter activity of LEDGF or αB-crystallin. CAT-ELISA was performed using *Prdx6*$^{-/-}$ cells overexpressed with PRDX6 following cotransfection with Hsp27, or αB-crystallin promoter or LEDGF promoter. The CAT activities of these genes were restored, comparable to that observed in *Prdx6*$^{+/+}$ cells (Figures 6b and 7A, c). Similar results were obtained with regard to Hsp27 promoter (data not shown). It is clear from the results that the PRDX6 plays a significant role in gene regulation. Notably, Western analysis results confirmed the recovery of αB crystallin protein expression in these cells (Figure 7C, lane3).

Bioactive TGFβ attenuates the DNA-binding activity of LEDGF in *Prdx6*$^{-/-}$ LECs

Based on a previous report by our group that TGFβ-mediated alterations in LECs result in loss of DNA-binding activity of LEDGF,[29] we predict that the DNA-binding affinity of LEDGF may be reduced in *Prdx6*$^{-/-}$ cells. To test this, we performed a

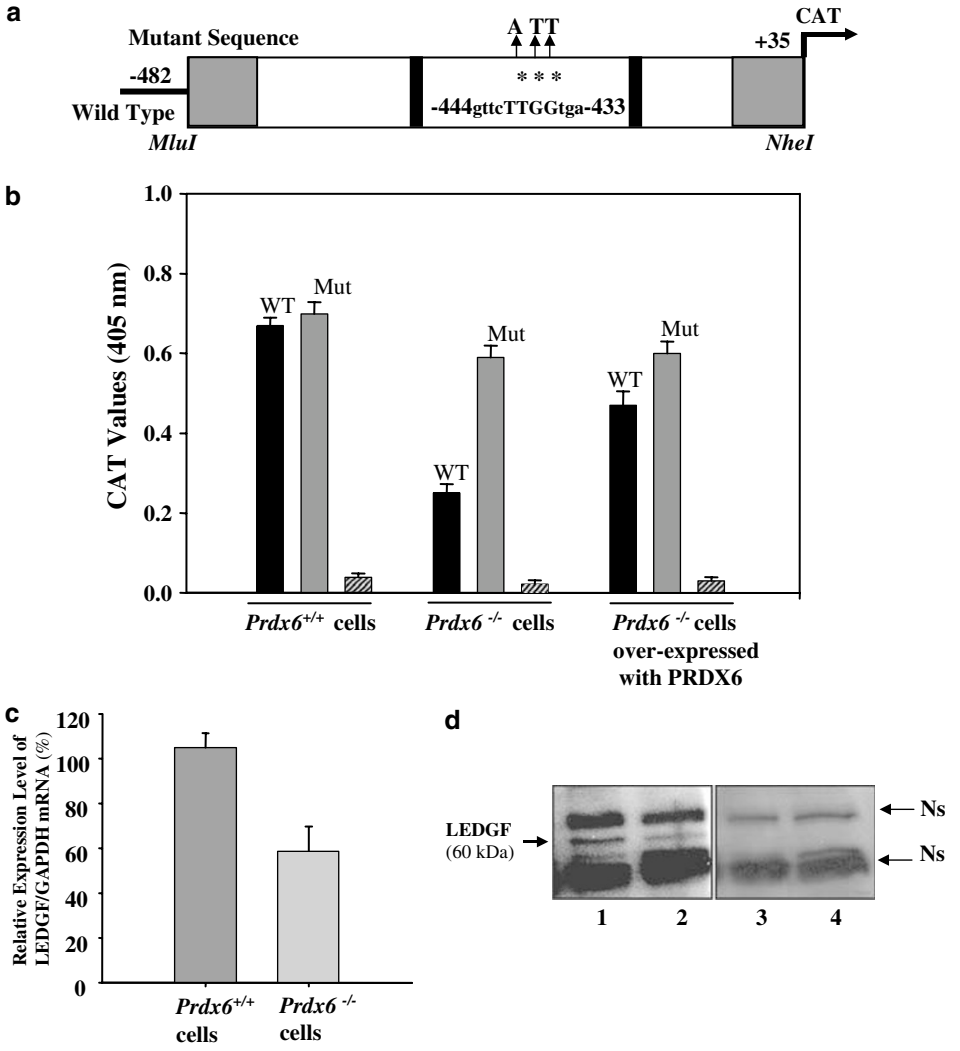

Figure 6 (**a**) Schematic representation of wild-type (having TIE) and mutated (where TIE is disrupted using site-directed mutagenesis) LEDGF promoter constructs. (**b**) Downregulation of promoter activity of LEDGF in *Prdx6*$^{-/-}$ cells. The cells were transiently transfected with LEDGF -CAT constructs and empty CAT vector and CAT-ELISA was performed after 72 h. CAT values in *Prdx6*$^{-/-}$ cells transfected with wild-type construct were significantly lower (black bars) than in *Prdx6*$^{+/+}$ cells; however, not much difference could be seen in cells with mutated construct (gray bars), indicating that downregulation of CAT values in *Prdx6*$^{-/-}$ cells is TGFβ-mediated suppression of promoter activity of LEDGF. Overexpression of PRDX6 restored promoter activity of LEDGF significantly (black bar). Empty CAT vector (stripped bars) has shown insignificant CAT activity. (**c**) Real-time PCR showing downregulated expression of LEDGF in *Prdx6*$^{-/-}$ cells. Total RNA was extracted from the cultured cells and reverse-transcribed into cDNA and real-time PCR was performed. The relative expression level of LEDGF was adjusted to that of GAPDH mRNA. (**d**) Western blot showing reduced expression of LEDGF in *Prdx6*$^{-/-}$ cells (lane 2). A band of 60 kDa denotes native LEDGF band that was knocked out when immunostained with neutralized LEDGF Ab. Ns are nonspecific bands that represent equal loading

gel-shift assay. Oligonucleotides containing LEDGF-binding sites, HSE and STRE, were synthesized,[29] and utilized for determining the DNA-binding affinity of LEDGF in nuclear extracts isolated from *Prdx6*$^{-/-}$ and *Prdx6*$^{+/+}$ LECs. LEDGF in nuclear extracts from *Prdx6*$^{-/-}$ cells displayed reduced binding, while that in nuclear extracts from *Prdx6*$^{+/+}$ cells formed a shifted band designated 'Cm1' (Figure 8a, lane 4) that supershifted to the 'Ss1' band after the addition of LEDGF-specific antibody (Figure 8a, lane 5). A band (Ns) appeared in all lanes with approximately the same intensity, signifying a nonspecific entity. This band was used to confirm equal loading, since it remained constant in nuclear extracts of both cell types. This signifies that not all nuclear proteins in *Prdx6*$^{-/-}$ cells lose their DNA-binding property. Additionally, the Cm1 band was outcompeted by 1000-fold excess of cold probe (Figure 8a, lanes 3 and 6), suggesting LEDGF-binding specificity. Similar results were obtained with a STRE probe (data not shown). Next, we wished to know whether *Prdx6*$^{+/+}$ cells exposed to TGFβ revealed reduced DNA-binding activity of LEDGF. We performed gel-shift assay using nuclear extracts isolated from these cells with HSE probe. We found that the binding activity of LEDGF is significantly reduced (Figure 8b, lanes 3 and 4). A similar finding has been reported earlier with hLECs treated with TGFβ1.[29] These results support that the ROS-mediated activation of TGFβ1 is responsible for this reduced binding that may be associated

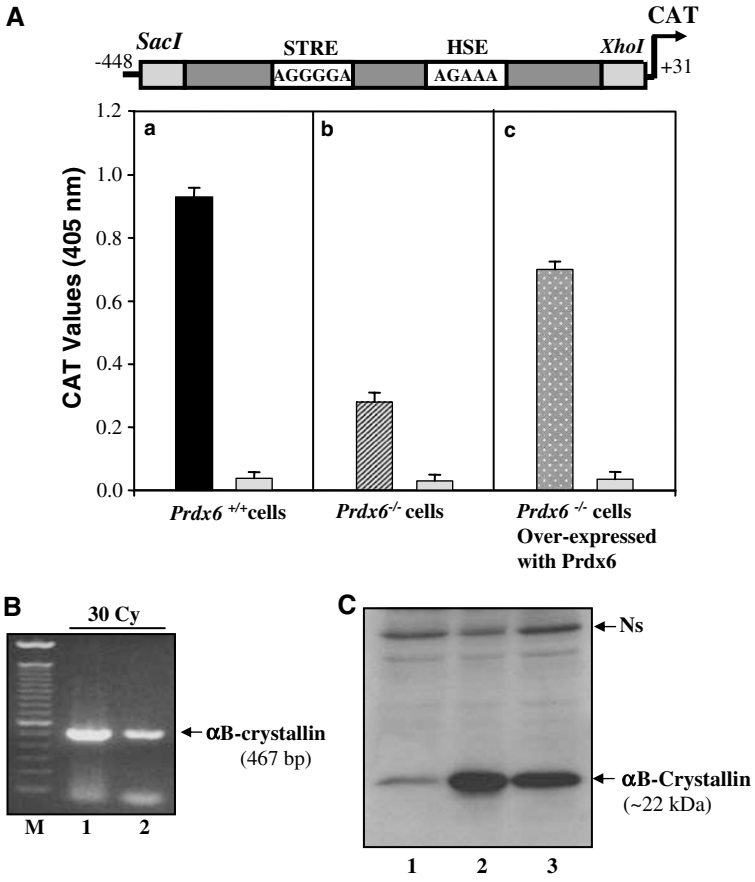

Figure 7 (**A**) Transcription repression of αB-crystallin promoter activity in *Prdx6*$^{-/-}$. The cells were transiently transfected with αB-crystallin-CAT constructs and empty CAT vector. After 72 h, CAT activity was assayed using CAT-ELISA. CAT values in *Prdx6*$^{-/-}$ cells were significantly lower than in *Prdx6*$^{+/+}$ cells (**b**; stripped bar) in comparison to *Prdx6*$^{+/+}$ cells (**a**; black bar). Overexpression of PRDX6 restored αB-crystallin promoter activity (**c**; dotted bar). Empty Cat vector (gray bars) has shown insignificant CAT activity. **B**. RT-PCR discloses reduced level of αB-crystallin mRNA in *Prdx6*$^{-/-}$ cells (lane 2). M represents DNA 100 bp marker. (**C**) Protein blot shows diminished level of αB-crystallin protein in *Prdx6*$^{-/-}$ cells (lane, 1) in comparison to *Prdx6*$^{+/+}$ cells (lane, 2). Overexpression with PRDX6 could restore the normal condition and the level of αB-crystallin protein in *Prdx6*$^{-/-}$ cells was comparable to *Prdx6*$^{+/+}$ cells (lane, 3). Ns denotes equal loading of protein samples

with either attenuation of LEDGF protein or lower abundance of protein.

To establish that supplying PRDX6 to *Prdx6*$^{-/-}$ cells recovers DNA-binding activity, nuclear extracts from LECs overexpressing PRDX6 were used in EMSA with the same probe. Our results suggest that a supply of PRDX6 to *Prdx6*$^{-/-}$ cells is able to restore the DNA-binding activity of LEDGF (Figure 8c, lane 1).

Prdx6$^{-/-}$ LECs overexpressing PRDX6 display normal LEC phenotype

PRDX6-depleted cells lose their *bona fide* phenotypes, and do not maintain homeostasis. We next determined whether expression of PRDX6 in *Prdx6*$^{-/-}$ cells could restore the normal phenotype of LECs, and affect the expression of α-SM actin, a biomarker for cataractogenesis. To this end, we performed multiple transfections, and selected stably transfected GFP-PRDX6 cells (Figure 9A, c and d). Cells were harvested and photomicrographed. In parallel experiments, *Prdx6*$^{+/+}$ cells were used as control. Interestingly, *Prdx6*$^{-/-}$ cells overexpressed with PRDX6 displayed normal phenotype, reduced α-SM actin expression, and limited apoptosis (Figure 9A, b). From the above findings, we conclude that PRDX6 is bifunctional. Specifically, it protects cells from oxidative stress, and controls ROS levels, thus playing a role in gene regulation. However, overexpression of LEDGF in *Prdx6*$^{-/-}$ LECs did not affect the phenotypic changes, suggestive of complex signaling. Our data support ROS-mediated activation of TGFβ, and TGFβ-induced changes in *Prdx6*$^{-/-}$ LECs, and a supply of PRDX6 may attenuate the ROS-mediated deleterious effects.

Discussion

ROS are associated with numerous cellular metabolic and signaling pathways, and play a role in disease, particularly age-related degenerative conditions, such as cataract. To date, catalase (CAT) and glutathione peroxidase (GPXs) have been viewed as the major enzymes responsible for removal of cytotoxic ROS. Our data now suggest that PRDXs also might play a more important role in controlling ROS levels. Indeed, it has been reported that CAT and GPXs can be inactivated by oxidative attack.[55,56] In this report, using LECs derived from mice with targeted inactivation of PRDX6, we show that PRDX6-deficient LECs display phenotypic

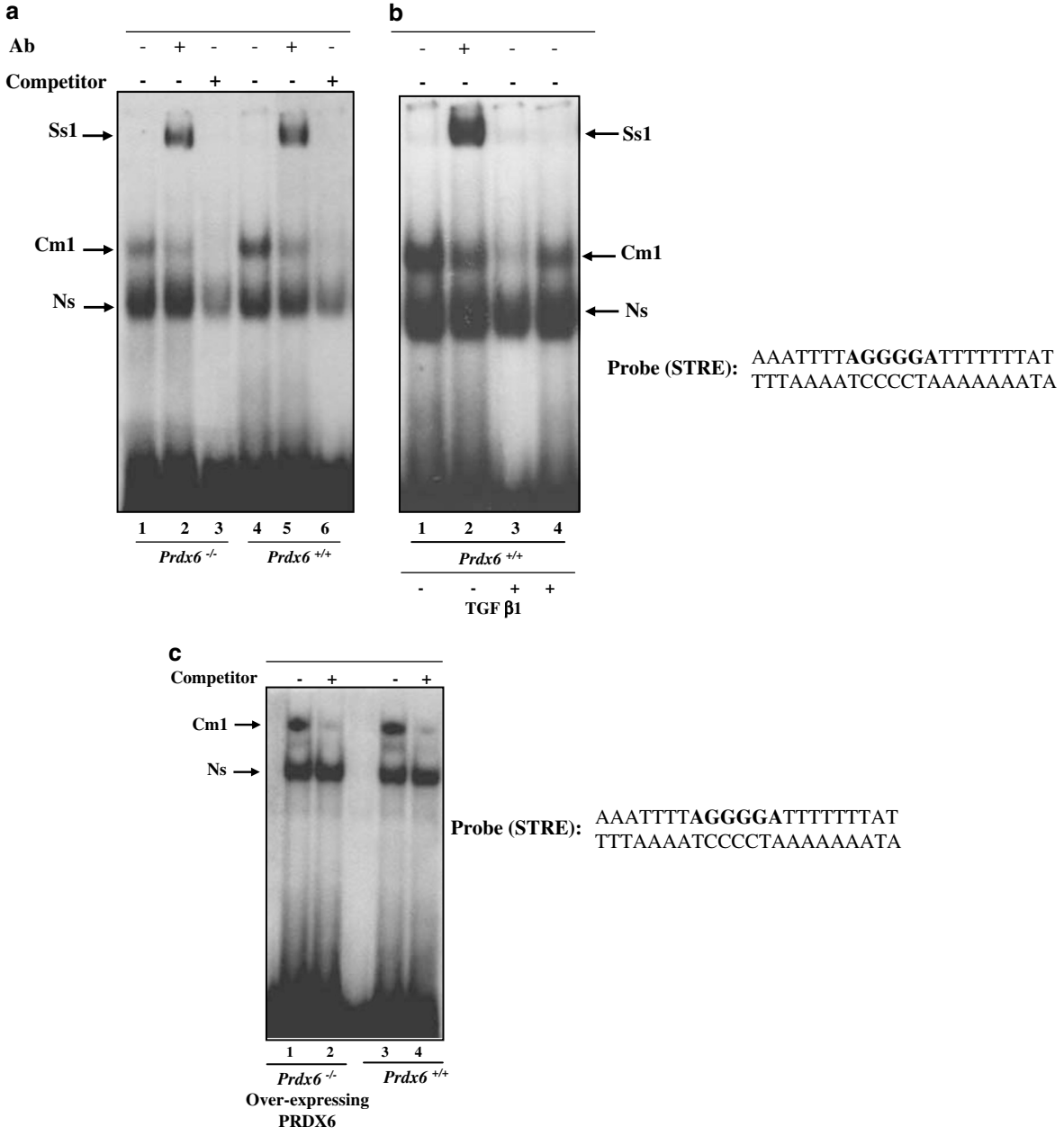

Figure 8 Gel shift and supershift assays showed attenuation of DNA-binding affinity of LEDGF in *Prdx6*$^{-/-}$ cells. (**a**) The Nuclear extract (2 μg) was incubated with radiolabeled probe having STRE-binding element ((A/T)GGGG(A/T)). A strong Cm1 band could be seen in *Prdx6*$^{+/+}$ cells (**a**; lane 4) that shifted to a higher molecular weight position shown by the Ss1 band (**a**; lane 5). On the other hand, nuclear extract from *Prdx6*$^{-/-}$ cells was also bound to the probe (lane1), but the binding was not as strong as in *Prdx6*$^{+/+}$ cells (**a**; lane 4), indicating TGFβ1-mediated reduction in DNA binding. Addition of unlabeled self-competitor at 1000-fold molar excess eliminated the Cm1 band (**a**; lane 3 & 6). (**b**) Nuclear extract (5 μg) isolated from *Prdx6*$^{+/+}$ cells treated with TGFβ1 at 5 ng/ml did not bind to the probe (**b**, lane 3) or binds weakly when treated at 2 ng/ml (**b**; lane 4). Untreated *Prdx6*$^{+/+}$ cells served as control showing, strong Cm1 band (**b**; lane 1) that supershifted after addition of LEDGF-specific antibody (**b**; lane 2). (**c**) Overexpression with PRDX6 restored the DNA-binding affinity of LEDGF to STRE element. Nuclear extract (2 μg) isolated from *Prdx6*$^{+/+}$ cells and *Prdx6*$^{-/-}$ cells overexpressing PRDX6 was incubated with radiolabeled probe. A strong Cm1 band could be seen in *Prdx6*$^{+/+}$ cells (**c**; lane 3) that was eliminated after addition of cold competitor (**c**; lane4). Cells overexpressing PRDX6 also showed strong Cm1 band (**c**; lane1), comparable to *Prdx6*$^{+/+}$ cells and was eliminated by the addition of self-competitor (**c**; lane2)

changes, spontaneous apoptosis, and enhanced expression of α-SM actin (a bio-marker for cataractogenesis). These changes of *Prdx6*$^{-/-}$ LECs are indistinguishable from those of TGFβ-induced changes in LECs.[29,44] In addition, these cells exhibit increased sensitivity to oxidative stress, and changes observed in PRDX6-deficient LECs involved higher ROS levels as assessed by H2-DCFH-DA staining (Figure 4A and C). We find that PRDX6 is a major antioxidant and vitally important to maintaining cellular integrity, and is highly expressed in mice lenses (Figure 1A). Our study demonstrates

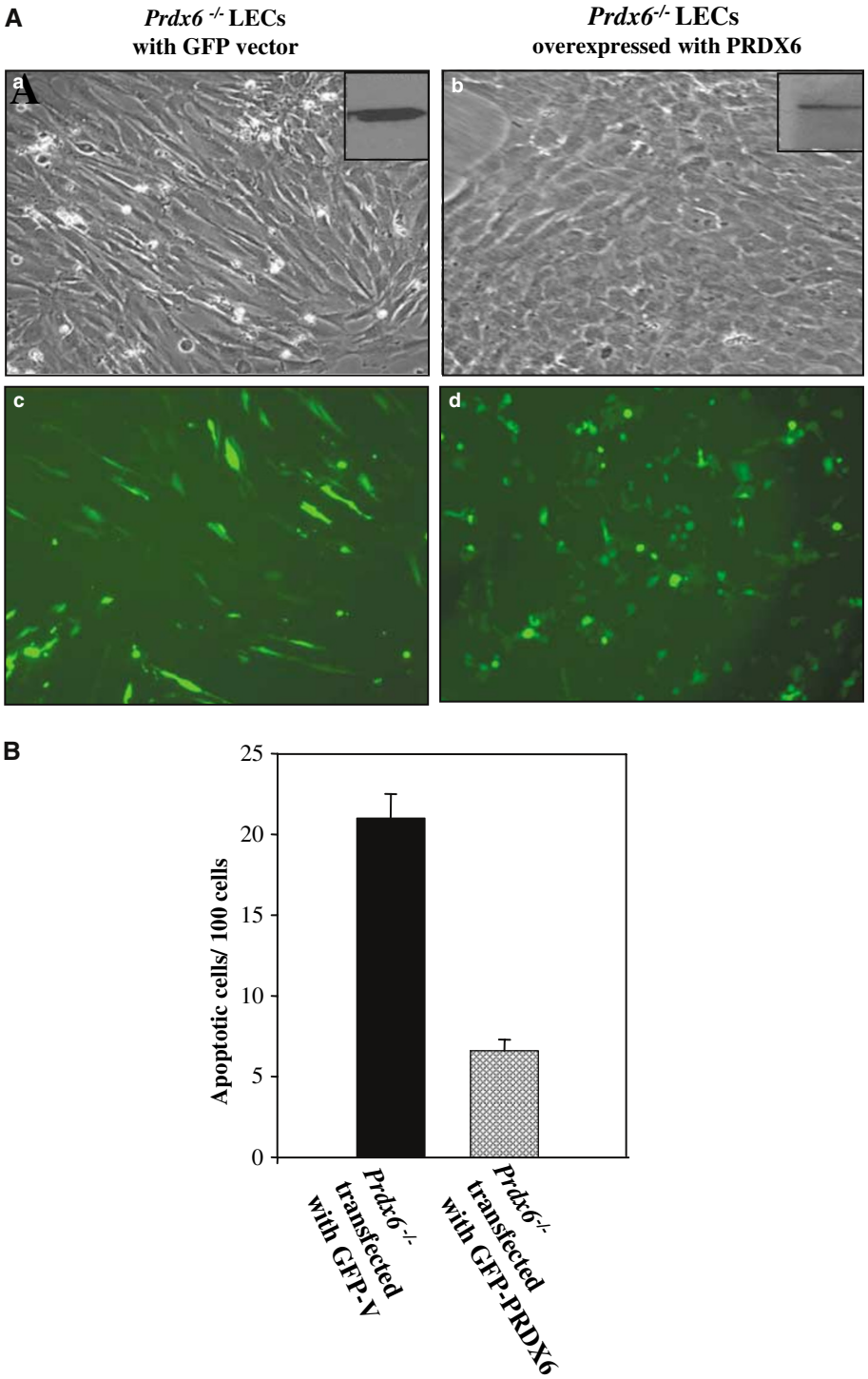

Figure 9 Effect of PRDX6 expression on apoptosis and phenotypic alterations and α-SM actin in *Prdx6*$^{-/-}$ LECs. *Prdx6*$^{-/-}$ LECs were cultured and stably transfected with pGFP-PRDX6 or GFP vector only as described in 'Materials and Methods' section. Cells were photomicrographed to compare phenotypic changes; GFP-vector-transfected LECs (**A**; **a** and **c**) and GFP-PRDX6-transfected LECs (**A**; **b** and **d**). Restoration of morphological structure can be seen (**A**; **b**), which are the typical phenotypes of LECs. Notably, Western analysis reveals the reduction in expression level of α-SM actin (**A**; **b**, right corner) compared to control (**A**; **a**, right corner). In addition, overexpression of PRDX6 could block apoptotic cellular death (**B**; dotted bar) compared to GFP-vector (**B**; Black bar)

that *Prdx6*$^{-/-}$ LEC death or cellular changes are prevented by the supply of PRDX6. PRDX6 inhibits ROS production, and thereby provides cytoprotection. The protective activity of PRDX6 is well comparable to that of MnTBAP. MnTBAP rescues cells from ROS-mediated cytotoxicity, possibly through mimicry of superoxide dismutase and/or

catalase.[57,58] Furthermore, TGFβ1 is increased and activated in *Prdx6*$^{-/-}$ LECs. This increase is abolished by a supply of PRDX6, indicating that ROS is the major cause of abnormality in *Prdx6*$^{-/-}$ LECs. Importantly, our finding indicates that the expression levels of PRDX5 are significantly higher than PRDX 1–4, but significantly lower than PRDX6. Since other PRDXs could not counteract the changes occurred in *Prdx6*$^{-/-}$ LECs and supply of PRDX6 could restore the abnormal changes in *Prdx6*$^{-/-}$ LECs, we consider the role of PRDX6 as major, at least in LECs. Furthermore, the presence of PRDX5 expression in LECs indicates that there is no balance between PRDX6 and PRDX5, since PRDX5 that exhibit cytosolic as well as mitochondrial localization could not be able to attenuate the abnormal changes in *Prdx6*$^{-/-}$ LECs. This absence of balance can be explained by the fact that PRDX6 might have other cellular function(s) in addition to its protective antioxidant activity. Indeed, PRDX6 has been implicated in signal transduction in mammalian cells, through control of ROS levels.[10] Recently, using *Prdx6*$^{-/-}$ mouse, it has been reported that endogenously produced mouse PRDX6 functioned *in vivo* as an antioxidant enzyme, and its function was not redundant to other PRDXs and antioxidant enzyme.[43] Notably, the gene expression of Prdx1–5, Gpx1–4, Cat, superoxide dismutase (Sod1–3), thioredoxin (Txn1–2), and Glutaredoxin (Glrx1–2) was found similar between *Prdx6*$^{-/-}$ and *Prdx6*$^{+/+}$ mice.[43] These findings suggest that PRDX6 activities are independent of other enzymes. Similarly, our results indicate that PRDX6-depleted cells were highly susceptible to oxidative stress and cells lacking this protein could not maintain cellular integrity. Thus, the present finding demonstrates that PRDX6 has unique properties and that it functions independently of other PRDXs and antioxidant proteins.

However, changes in the redox state of cells lead to the modification of cellular signaling molecules, including transcription factors and proteins involved in protection. Diminished cellular antioxidant levels place cells in the redox state, which induces redox-active genes, and results in hyperactivity. In the present study, the possible biological role of the oxidized state in gene expression was investigated using LEDGF, a survival factor, and its regulated genes, αB-crystallin, hsp27, and TGFβ-inducible gene. LEDGF is responsive to TGFβ and ROS.[21,29] Activation of TGFβ by ROS is well established.[30,35,36] Our data strongly support the presence of bioactive TGFβ in culture media of *Prdx6*$^{-/-}$ *LECs* (Figure 5c). TGFβ is present in ocular media, and various levels of TGFβ activity have been reported in aqueous and vitreous in human and other species.[59,60] Interestingly, increased levels of H_2O_2 in aqueous humor are associated with cataractogenesis.[34,61,62] We believe that ROS enhances the expression and activation of TGFβ, which negatively regulates survival pathway(s) in LECs by attenuating gene transcription. Moreover, lens-specific expression of TGFβ1 in transgenic mice induces anterior subcapsular cataracts.[46] These include phenotypic changes, apoptosis, and expression of α-SM actin, similar to those observed in human cataract. Interestingly, if TGFβ is injected into the vitreous or aqueous chamber of rat eye *in vivo,* the most pronounced changes occur at the bow region of the lens, initiating more typical cortical cataract. Our present results show that lenses from *Prdx6* knockout mice are highly susceptible to oxidative stress, and develop cataracts (opacity) and abnormal migration of LECs from the bow to posterior region (Figure 1C). These findings suggest the possible involvement of TGFβ in cataractogenesis induction. In addition, we find the expression of βig-h3 protein in *Prdx6*$^{-/-}$ LECs (Figure 2B). βig-h3 is inducible by TGFβ,[63,64] and its overexpression is implicated in anterior polar cataract.[65] Thus, the induction of βig-h3 in *Prdx6*$^{-/-}$ LECs further supports our hypothesis. However, the functions of βig-h3 in lens pathology remain to be investigated. Nevertheless, higher levels of ROS play a role in the aging process, as well as in a number of human diseases, including age-related cataractogenesis. On the basis of data obtained from our system *(Prdx6*$^{-/-}$ cells), we predict the overstimulation of normal ROS-regulated signaling pathways in *Prdx6*$^{-/-}$ cells. We consider that ROS increases in LECs during aging due to deficiency of PRDX6. Thus, during aging, TGFβ is activated by ROS, and further enhances ROS production by diminishing level of PRDX6 expression, which results in negative regulation of the survival pathway(s) in LECs due to attenuation of gene transcription. However, in support of this view further investigation is required.

Oxidative stress may modify the DNA-binding activity of LEDGF, similar to *Prdx6*$^{-/-}$ cells. To achieve biological effects, the transcription factor, LEDGF, binds to HSE and STRE present in stress-associated genes. High level of ROS (*Prdx6*$^{-/-}$ cells) may activate or repress LEDGF, and may attenuate binding to DNA. We found the DNA-binding activity of LEDGF is reduced in *Prdx6*$^{-/-}$ LECs (Figure 8a and b). In addition, the results of Figure 8c show that PRDX6 inhibit the attenuation of DNA-binding activity of LEDGF to HSE and STRE. However, based on our present study and other's reports, it is pertinent to question how PRDX6 can play the roles of cell death and cell survival. Although we do not yet know the complete answer to this question, evidence indicates that it does so by the modulation of gene transcription by controlling ROS. In the present study, we found that *LEDGF* gene transcription and protein expressions were downregulated in *Prdx6*$^{-/-}$ LECs (Figure 6). Interestingly, a similar result has been obtained when human LECs were exposed to TGFβ.[29] On the basis of these results, we surmise that there may be two possible mechanisms for ROS mediated-TGFβ1 inhibition of LEDGF expression. First, bioactive TGFβ1 may act at the TIE site present in *LEDGF* gene (Figure 6b) through c-fos[27] and dominantly repress the positive signal. We found that the negative regulation of *LEDGF* gene is associated with the presence of TIE in the *LEDGF* gene (Figure 6b). Second, there is a possibility of attenuation of DNA-binding activity of LEDGF either due to lower abundance of LEDGF protein or its attenuation in *Prdx6*$^{-/-}$ cells. Moreover, we also consider the simultaneous presence of both events in these cells. We believe the deactivation of LEDGF protein in *Prdx6*$^{-/-}$ cells, perhaps due to the prevalence of activated caspases. LEDGF is cleaved by caspase-3 and -7 during apoptosis.[66] Wu *et al*.[66] have reported that LEDGF was cleaved during apoptosis into fragments of 65 and 58, and this protein bears three sites: DEVPD30 G, DAQD486 G, and WEID85. Thus, it is possible that the LEDGF prosurvival function is abolished in PRDX6-depleted cells. There is evidence that full-length LEDGF

enhances resistance of cells against oxidative and thermal stress by upregulating the expression of stress-related, antiapoptotic proteins, such as hsp27, αB-crystallin, and PRDX6.[17,25,67–71]

Moreover, under normal physiological conditions, LEDGF is a regulator of PRDX6.[17] Attenuation of LEDGF function in cells with higher ROS levels should subsequently lead to decreased production of PRDX6.[17] Repression of LEDGF transcription in PRDX6-depleted LECs may be due to the prevalence of bioactive TGFβ (Figure 5c). As mentioned above, LEDGF promoter bears TIE, a target for transcriptional repression of LEDGF by TGFβ.[29] A CAT assay using the LEDGF promoter containing TIE[27–29] is activated in the presence of PRDX6, suggesting that the PRDX6 disrupts harmful ROS-mediated TGFβ1 signaling. In addition, the expression levels of αB-crystallin are recovered (Figure 7). The recovery of LEDGF function, as well as restoration of phenotype *in Prdx6*$^{-/-}$ LECs by the addition of PRDX6, further supports the involvement of ROS-mediated signaling. However, *Prdx6*$^{-/-}$ LECs overexpressing LEDGF did not restore the phenotype of *Prdx6*$^{-/-}$ LECs (data not shown). This result suggests the involvement of other ROS-mediated dominant signals that need to be investigated. However, collectively, our data indicate that LEDGF prosurvival function is attenuated due to higher prevalence ROS in *Prdx6*$^{-/-}$ cells and activation of TGFβ. This leads to the reduced expression of antiapoptotic genes such as *Hsp27* and *αB-crystallin* and *Prdx6.*[17,29] Recent reports provide evidence that redox regulation is a general mechanism for post-translational control of transcription factor function. Changes in the reduction–oxidation potential influence the DNA-binding activities of several transcription factors, including AP1, NF-κB, and HSF1.[72,73] Various harmful signals by ROS have been reported in aged cells.[31–33,42] We believe that the *Prdx6*$^{-/-}$ LECs used in this study may represent a model that can be used to elucidate the signaling pathways involved in aged cells. Furthermore, our results show that reduction in transcription and attenuation of the DNA-binding activity of LEDGF are largely associated with ROS activation of TGFβ in *Prdx6*$^{-/-}$ LECs. In summary, oxidative stress is a major cause of cell damage associated with the initiation and progression of many age-related degenerative diseases, including cataractogenesis. In the majority of organisms, from prokaryotes to eukaryotes, cells have evolved antioxidant defense systems that rapidly nullify harmful oxidants. Thus, our findings demonstrate that PRDX6 is pivotal in maintaining cellular homeostasis by protecting cells from oxidative stress and playing a role in signaling.

Materials and Methods

Generation, characterization and breeding of *Prdx6*-targeted mutant mice

The generation, characterization, mating of mutant mice, and analysis of the progeny of *Prdx6* targeted mutant mice has been described in detail.[74,75,43] Briefly, a genomic clone having the 129/SvJ (129) *Prdx6* gene was isolated as described previously.[75] *Prdx6*$^{-/-}$*129/Sv* mice were generated in Harvard Medical School under the supervision of Dr. David R Beier. These mice are maintained on a fully inbred 129/Sv background, which minimizes the variation due to genetic background. However, to generate the *Prdx6-targeted* mutant mice of 129/SvJ (129) background, the chimeric *Prdx6-targeted* mutants were crossed to 129 mice, and those offsprings heterozygous for the *Prdx6-targeted* mutation were intercrossed to generate mice homozygous for the targeted Prdx6 gene mutation. *Prdx6*$^{-/-}$ mutant mice of pure 129 background were used during the present study. Wild-type 129/SvJ inbred mice of the same sex and age were used as control (*Prdx6*$^{+/+}$).

Mutant genotypes of *Prdx6*$^{-/-}$ were confirmed by PCR of genomic DNA obtained from the tail.[43] All animals were maintained under specific pathogen-free conditions in the animal house at Harvard Medical School. Mice lacking PRDX6 developed normally. There was no difference among the age- and sex-matched body weights of adult homozygous and heterozygous mutants, and wild-type controls. Microscopically, no abnormalities were found in any of the organs and tissues of mutants and their controls.[43]

LECs and Lens organ culture

Lenses were isolated from 7–8-weeks-old mice, and *Prdx6*$^{-/-}$ and *Prdx6*$^{+/+}$ cell lines were generated and maintained in Dulbecco's Modified Eagle's (DMEM) with 10% FBS.[76] Briefly, cells were cultured in 75 mm tissue culture flasks in a 5% CO2 environment at 37°C following standard procedures. Cells were trypsinized (0.25%) and plated in culture dishes at a density of 5×10^5 in 60 mm plates or 1×10^6 in 100 mm plates when required. All transfection procedures were performed using Superfectamine (Qiagen). For treatment with TGFβ1 (R&D systems, Minneapolis), H_2O_2 or MnTBAP, cells were cultured in 24- or 96-well plates.

Lenses from *Prdx6*$^{-/-}$ (homozygous) and *Prdx6*$^{+/+}$ (wild-type) 8-month-old mice were placed in Medium 199 (Gibco) after removal from mouse eyes subjected to oxidative stress.[76] Lenses were photographed using a slit lamp and dissection microscope, following H_2O_2 exposure. For histopathological evaluation, lenses from both groups of mice were fixed in 4% paraformaldehyde in 20 mM phosphate-buffered saline, pH 7.4, embedded in paraffin, and cut into 5 μm sections. Sections were deparaffinized with xylene, passed through a graded series of alcohol, and finally stained with Meyer's hematoxylin and eosin (Sigma) using a standard technique,[77] and photomicrographed.

Cell survival assay (MTS assay)

A colorimetric MTS assay (Promega) was performed as described earlier.[78] This assay of cellular proliferation uses 3-(4,5-dimethylthiazol-2-yl)-5-(3-carboxymethoxyphenyl)-2 to 4-sulfophenyl)-2H-tetrazolium salt (MTS; Promega, Madison, MI, USA). Upon addition to medium containing viable cells, MTS is reduced to a water-soluble formazan salt. The $OD_{490\,nm}$ value was measured after 4 h with an ELISA reader.

Apoptotic cell assay

DAPI staining was performed as described elsewhere.[79] Briefly, cells were grown in complete medium overnight and the next day, washed once with PBS, and fixed in 70% ethanol. Cells were re-washed with PBS, incubated in DAPI solution for 30 min at room temperature, washed, and mounted. The morphology of cell nuclei was observed under a fluorescent microscope, following UV excitation at 350 nm. After photomicrography, apoptotic nuclei were identified by condensed chromatin gathering at the periphery of the nuclear membrane or total fragmented morphology of

nuclear bodies, when *Prdx6*$^{-/-}$ cells were compared with *Prdx6*$^{+/+}$ cells.

A TUNEL assay was employed to assess apoptotic cell death. TUNEL staining was performed using an *in situ* cell death detection kit, Fluorescein (Roche Diagnostics GmbH, Germany), following the company's protocol. Briefly, cells were washed with PBS and fixed in freshly prepared 4% paraformaldehyde in PBS (pH 7.4), followed by incubation in permeabilization solution (0.1% Triton X-100, 0.1% sodium citrate) for 2 min on ice. Cells were rinsed twice with PBS, and incubated in a TUNEL reaction mixture for 60 min at 37°C in the dark. Cells were rinsed three times with PBS. After mounting, samples were micro-photographed using a microscope (Nikon, ECLIPSE TE 300), and analyzed.

Western blot analysis

Cell lysates were prepared in ice-cold radioimmune precipitation buffer (RIPA buffer), as described previously.[17] Equal amounts of protein samples were loaded onto a 10% SDS gel, blotted onto PVDF membrane (Immobilon™-P; Millipore Corporation, Bedford, MA, USA), and immunostained with primary antibodies at the appropriate dilutions (mouse anti-α-SM actin at 1 : 400 dilution (Sigma), αB-crystallin or αA-crystallin antibody (1 : 500) (a kind gift from Dr Jack Liang, Harvard Medical School, Boston), HSP27 (Santacruz Biotech) (1 : 1000), TGFβ1 antibody (Santacruz Biotech) (1 : 400) or anti-TGFβ-inducible gene (1 : 1000) (a kind gift from Dr. Paul C Billings, Univ. Pennsylvania School of Medicine, Philadelphia). Filters were incubated with horseradish peroxidase-conjugated secondary antibodies (1 : 1500 dilution). Specific protein bands were visualized by incubating the membrane with luminol reagent (Santa Cruz Biotechnology) and exposing to film (X-OMAT; Eastman Kodak).

Real-time PCR

To monitor the levels of PRDXs in mouse lens, total RNA was isolated using the single-step guanidine thiocynate/phenol/chloroform extraction method (Trizol Reagent;Invitrogen) and converted to cDNA using Supercsript II Rnase H$^-$ Reverse Transcriptase. Quantitative real-time PCR was performed with TaqMan Universal Master Mix (Applied Biosystems, Foster City, CA, USA) in an ABI® 7000 Sequence detector system (Applied Biosystems). We used primers specific for *Prdx 1*[43] (forward, 5′-ACACCCAAGAAACAAGGAGGATT-3′ and reverse, 5′-CAACGGGAAGATCGTTTATTGTTA-3′), *Prdx2* (forward, 5′-AACGCGCA AATCGGAAAGT-3′ and reverse, 5′-AGTCCTCAGCA TGGTCGCTAA-3′), *Prdx 3* (forward, 5′-GGCCACATGAACATCACACTGT-3′ and reverse, 5′-CAAACTGGAACGCCTTTACCA-3′), *Prdx 4* (forward, 5′-TCCTGTT GCGGACCGAAT-3′ and reverse, 5′-GAAAGAAGCAGGTTGGGAGTGT-3′), *Prdx 5* (forward, 5′-GAAAGAAGCAGGTTGGGAGTGT-3′ and reverse, 5′-CCCAGGGACTCCAAACAAAA-3′), and *Prdx 6* (forward, 5′-TTGATGA TAA GGG CAGGGAC-3′ and reverse, 5′-CTACCATCACGCTCTCTCCC-3′). The mRNA levels of each *Prdx* were adjusted to the mRNA copies of β-actin.

Reverse transcription polymerase chain reaction (RT-PCR)

RT-PCR was conducted following an earlier method.[21] A TGFβ1-specific primer pair (Cat. no. RDP-26-025) was purchased from R&D Systems (Minneapolis, MN, USA). Other primers were synthesized commercially (Invitrogen). To perform RT-PCR, either total RNA or mRNA was extracted from *Prdx6*$^{-/-}$ and *Prdx6*$^{+/+}$ cells using the single-step guanidine thiocyanate–phenol–chloroform extraction method (Trizol Reagent; GIBCO-BRL), and isolated with the Micro-fast track™ kit (Invitrogen, Carlsbad, CA, USA). Micro-fast track 2 (Invitrogen, Carlsbad, CA, USA), a cDNA synthesis kit for RT-PCR, was employed to synthesize cDNA from mRNA. The resulting cDNA was used for amplification. After denaturation for 2 min at 95°C, 30 cycles of amplification (denaturation at 94°C for 1 min, annealing at 55°C for 2 min, elongation at 72°C for 3 min) were performed, followed by a final extension step for 7 min at 72°C. The following oligonucleotide sequences were employed: LEDGF sense primer: 5′-AAC ACA CAG AGA TGA TTA CTA CAC-3′, LEDGF antisense primer: 5′-TTT CAA CAT CAA ACC TAT GCT TAT-3′, encompassing the full-length 524 bp open reading frame of LEDGF, αB-crystallin sense primer, 5′-ATGGACATCGCCATCCACCA-3′ and antisense primer, 5′-GACAGCAGGCTTCTCTTCAC-3′ covering 467 bp of the open reading frame of mouse αB-crystallin, and mouse TGFβ-inducible gene (βig-h3)[80] sense primer, 5′-GGA AGG CTG TCA TCT CCA AC-3′ and antisense primer, 5′-CTC CGC TAA CCA GGA TTT CA-3′ (702 bp).

Construction of LEDGF promoter–CAT reporter vector

The 5′-flanking region of the *LEDGF* gene was isolated and sequenced. A construct encompassing -5139 to $+35$ bp was prepared by ligation to basic pCAT vector (Promega, Madison, WI, USA). Similarly, constructs containing different sizes of the LEDGF promoter were prepared with the appropriate sense and antisense primers, and ligated to pCAT vector.[29] The plasmid was amplified, and used for the CAT assay. In this study, we employed a construct comprising bases -482 to $+35$, which included TIEs. Additionally, we used a mutated construct in which the TIE site is disrupted.[29]

Construction of Hsp27 and αB-crystallin-CAT

Hsp27-CAT and αB-crystallin-CAT constructs were engineered as described previously.[25] Briefly, the 5′-flanking region of the human *Hsp27* gene was isolated with a genomic PCR kit (Clontech, Palo Alto, CA, USA) using specific primers. A forward primer containing a *Sac*I site (5′-GCGTCGAGCTCTCGAATTCATTTGCTT-3′) and reverse primer with a *Xho*I site (5′-GCTCTCGAGGTCTGCTCAGAAAAGTGC-3′) were used to generate the fragment, which was cloned between the *Eco*RI sites of the TA vector (Invitrogen Corp., Carlsbad, CA, USA). Similarly, a fragment comprising the 5′-flanking region of the human αB-crystallin promoter (a gift from Dr. Piatigorsky, NEI, NIH) was prepared using specific primers. A forward primer with a *Sac*I site (5′-CTCTCTTCCAAGAGCTCACAAAG-3′) and reverse primer containing a *Xho*I site (5′-ATGGTGGCTACTCGA GAGTGA-3′) were used to generate the above fragment, which was cloned between the *Eco*RI sites of the TA vector. The Hsp27 and αB-crystallin/TA constructs were digested with *Sac*I and *Xho*I and promoter fragments were ligated to pC AT-Basic vector (Promega, Madison, WI, USA), using the appropriate restriction enzymes.[25]

Transfection and chloramphenicol acetyltransferase assay (CAT assay)

The CAT assay was performed using a CAT-ELISA (Roche Diagnostics GmbH, Germany) kit. *Prdx6*$^{-/-}$and *Prdx6*$^{+/+}$ cells were cultured at a density of 5×10^5 cells in 5 ml DMEM containing 10% FBS per 60 mm petri dish in a 37°C incubator containing 5% CO2. After 24 h, cells were

washed with the same medium and transfected/co-transfected with Lipofectamine PLUS Reagent (Invitrogen) using 2 μg of promoter/CAT reporter construct and/or pEGFP expression vector, and 1 μg of SEAP vector.[81] After 72 h of incubation, cells were harvested, and extracts were prepared and normalized. CAT-ELISA was performed to monitor CAT activity, following the manufacturer's protocol. Absorbance was measured at 405 nm using a microtiter plate ELISA reader.

Assay for intracellular redox state

Intracellular redox state levels were measured using the fluorescent dye, H2-DCFH-DA, a nonpolar compound that is converted into a polar derivative (DCFH) by cellular esterases following incorporation into cells. H2-DCFH is rapidly oxidized to the highly fluorescent 2′,7′-dichloroflourescein in the presence of intracellular hydrogen peroxide and peroxidases.[35] For the assay, the medium was replaced with Hank's solution containing 10 μM H2-DCFH-DA after 10 min of incubation at room temperature. Cells were photomicrographed under an inverted fluorescent microscope at an excitation wavelength of 513 nm. The relative fluorescent intensity was measured in control cells.

Detection of biologically active TGFβ1

Bioactive TGFβ1 in culture supernatant was determined directly using the TGFβ1Emax ImmunoAssay system (Promega Corp., Madison, WI, USA).[33] Briefly, 96-well plates were coated with TGFβ Coat mAb, which binds to soluble TGFβ1. TGFβ1 bound to a specific polyclonal antibody (pAb). After washing, the amount of specifically bound pAb was measured using a specific antibody conjugated to HRP. Readings were taken at 450 nm.

Construction of PRDX6 in a eukaryotic expression vector

A construct containing green fluorescent protein (TOPO-GFP) and PRDX6 cDNA was generated with the 'living color system' (CLONTECH, Palo Alto, CA, USA) for eukaryotic expression. PRDX6 cDNA was isolated from the LEC library using sense and antisense primers,[17] and the amplified product was cloned into the TOPO-GFP vector. This construct was employed to generate stable eukaryotic cells overexpressing PRDX6 (GFP-PRDX6). Cells transfected with empty GFP vector served as a control.

Preparation of LEC nuclear and cytosolic extracts

Nuclear extracts from *Prdx6*$^{-/-}$ and *Prdx6*$^{+/+}$ cells were prepared as described earlier.[17] Briefly, cells were cultured in 100 mm plates. Next, cells were washed gently with chilled PBS (pH 7.2), collected by centrifugation, and resuspended in five pellet volumes of cytoplasmic extraction buffer (10 mM HEPES, 60 mM KCl, 1 mM EDTA, 0.075% (v/v) Nonidet P-40, 1 mM phenylmethylsulfonyl fluoride, adjusted to pH 7.6). After short incubation on ice, the cytoplasmic extract was removed from the pellet. Following careful washing with cytoplasmic extract buffer without detergent (Nonidet P-40), fragile nuclei were re-suspended in nuclear extract buffer (20 mM Tris-HCl, 420 mM NaCl, 1.5 mM $MgCl_2$, 0.2% EDTA, 1 mM phenylmethylsulfonyl fluoride, and 25% (v/v) glycerol, adjusted to pH 8.0). The salt concentration was adjusted to 400 mM using 5 M NaCl, and the extract was incubated on ice for 10 min with occasional vortexing. Finally, the extract was centrifuged at 14 000 rpm for 30 min to pellet the nuclei. After dialysis, protein concentration was estimated according to the Bradford method,[82] and the extract was employed for EMSA.

Electrophoretic mobility shift assay (EMSA)

In the present study, we performed EMSA with nuclear extracts from *Prdx6*$^{-/-}$ or *Prdx6*$^{+/+}$ cells to determine whether the DNA-binding property of LEDGF is attenuated in *Prdx6*$^{-/-}$ cells. Oligonucleotides containing HSE (nGAAn) and STRE (T/AGGGGA/T) were synthesized chemically (Gibco). Sequences were annealed, and end-labeled with [γ-^{32}P]ATP using T4 polynucleotide kinase (New England Biolabs, Inc.). The binding reaction was performed in 20 μl buffer containing 20 mM Tris-HCl (pH 8.0), 75 mM KCl, 5% glycerol, 50 μg/ml bovine serum albumin (BSA), 0.025% nonidet NP-40, 1 mM EDTA, 5 mM DTT, and 1 μg of poly(dI/dC). The end-labeled probe (5 fmol (1000 cpm)) was incubated on ice for 30 min with 5 μg of nuclear extract. Samples were loaded on a 5% polyacrylamide gel in 0.5 $\times$ TBE buffer for 2 h at 10 V/cm. The gel was dried and autoradiographed. In competition assays, a 1000-fold molar excess of cold probe was added. For the supershift assay, 1 μl of anti-LEDGF antibody (Ab) was added to the tube containing the probe and nuclear extract. The mixture was incubated for an additional 30 min while the complexes formed, and EMS A was performed, as described earlier.[17,25]

Acknowledgements

Grants provided by the National Eye Institute (EY-13394) (to DPS) and Fight For Sight (GA04048) to NF, and Foundation for Fighting Blindness are gratefully acknowledged.

References

1. Kehrer JP (1993) Free radical as mediators of tissue injury and disease. Crit. Rev. Toxicol. 23: 21–48
2. Kang SW, Baines IL and Rhee SG (1998a) Characterization of a mammalian peroxiredoxin that contains one conserved cysteine. J. Biol. Chem. 273: 6303–6311
3. Chae HZ, Robison K, Poole B, Church G and Storz G (1994) Cloning and sequencing of thiol-specific antioxidant from mammalian brain: alkyl hydroperoxide reductase and thiol-specific antioxidant define a large family of antioxidant enzymes. Proc. Natl. Acad. Sci. USA 91: 7017–7021
4. Hofmann B, Hecht HJ and Flohe L (2002) Peroxiredoxins. Biol. Chem. 383: 347–364
5. Jin DY and Jeang KT (2000) Peroxiredoxins in cell signaling and HIV infection In *Antioxidant and Redox Regulation of Genes*, Sen CK *et al.* (eds) (New York: Academic Press) pp 381–407
6. Peshenko I V and Shichi H (2001) Oxidation of active center cysteine of bovine 1-*cys* peroxiredoxin sulfenic acid form of peroxide and peroxynitrite. Free Radic. Biol. Med. 31: 292–303
7. Rabilloud T, Heller M, Rigobello MP, Bindoli A, Aebersold R and Lunardi J (2001) The mitochondrial antioxidant defense system and its response to oxidative stress. Proteomics 1: 1105–1110
8. Kinnula VL, Lehtonen S, Sormunen R, Kaarteenaho-Wiik R, Kang SW, Rhee SG and Soini Y (2002) Overexpression of peroxiredoxins I, II, III, V and VI in malignant mesothelioma. J. Pathol. 196: 316–323
9. Rabilloud T, Heller M, Gasnier F, Luche S, Rey C, Aebersold R, Benahmed M, Louisot P and Lunardi J (2002) Proteomics analysis of cellular response to oxidative stress: evidence for *in vivo* overoxidation of peroxiredoxins at their active site. J. Biol. Chem. 277: 19396–19401
10. Wood ZA, Poole LB and Karplus PA (2003a) Peroxiredoxin evolution and the regulation of hydrogen peroxide signaling. Science 300: 650–653

11. Woo HA, Chae HZ, Hwang SC, Yang KS, Kang SW, Kim K and Rhee SG (2003) Reversing the inactivation of peroxiredoxins caused by cysteine–sulfinic acid formation. Science 300: 653–656
12. Wood ZA, Schroder E, Harris JR and Poole LB (2003b) Structure, mechanism and regulation of peroxiredoxins. Trends Biochem. Sci. 28: 32–40
13. Link AJ (1997) Comparing the predicted and observed properties of proteins encoded in the genome of *Escherichia coli* K-12. Electrophoresis 18: 1259–1313
14. Lyu MS, Rhee SG, Chae HZ, Lee TH, Adamson MC, Kang SW, Jin DY, Jeang KT and Kozak CA (1999) Genetic mapping of six mouse peroxiredoxin genes and fourteen peroxiredoxin related sequences. Mamm.Genome 10: 1017–1019
15. Ellis HR and Poole LB (1997) Roles of the two cysteine residues of AhpC in catalysis of peroxide reductase by alkyl hydroperoxide reductase from *Salmonella typhimurium*. Biochemistry 36: 13349–13356
16. Choi HJ, Kang SW, Yang CH, Rhee SG and Ryn SE (1998) Crystal structure of a novel human peroxidase enzyme at 2.0 A resolution. Nat. Struct. Biol. 5: 400–406
17. Fatma N, Singh DP, Shinohara T and Chylack Jr. LT (2001) Transcriptional regulation of antioxidant protein2 gene, a thiol-specific antioxidant, by lens epithelium-derived growth factor to protect cells from oxidative stress. J. Biol. Chem. 276: 48899–48907
18. Pedrajas JR, Miranda-Vizuete A, Javanmardy N and Gustafsson J-A (2000) Mitochondria of *Saccharomyces cerevisiae* contain one-conserved cysteine type peroxiredoxin with thioredoxin peroxidase activity. J. Biol. Chem. 275: 16296–16302
19. Kim K, Kim IH, Lee KY, Rhee SG and Stadtman ER (1988) The isolation and purification of a specific 'Protector' protein which inhibits enzyme inactivation by a thiol/Fe (III)/O2 mixed-function oxidation system. J. Biol. Chem. 263: 4704–4711
20. Kim H, Lee T-H, Park ES, Suh JM, Park SJ, Chung HK, Kwon O-Y, Kim YK, Ro HK and Shong M (2000a) Role of peroxiredoxins in regulating intracellular hydrogen peroxide and hydrogen peroxide-induced apoptosis in thyroid cells. J. Biol. Chem. 275: 18266–18270
21. Sharma P, Singh DP, Fatma N, Chylack Jr. LT and Shinohara T (2000) Activation of LEDGF gene by thermal and oxidative stress. Biochem. Biophys. Res. Commun. 276: 1320–1324
22. Rhee SG (1999) Redox signaling: hydrogen peroxide as intracellular messenger. Exp. Mol. Med. 31: 53–59
23. Ge H, Si Y and Roeder RG (1998a) Isolation of cDNAs encoding novel transcription coactivators p52 and p75 reveals an alternate regulatory mechanism of transcriptional activation. EMBO J. 17: 6723–6729
24. Ge H, Si Y and Wolffe AP (1998b) A novel transcriptional coactivator, p52, functionally interacts with the essential splicing factor ASF/SF2. Mol. Cell 2: 751–759
25. Singh DP, Fatma N, Kimura A, Chylack Jr. LT and Shinohara T (2001) LEDGF binds to heat shock and stress-related element to activate the expression of stress-related genes. Biochem. Biophys. Res. Commun. 283: 943–955
26. Kubo E, Fatma N, Sharma S, Shinohara, Chylack Jr. LT and Singh DP (2002) Transactivation of Involucrin, a marker of differentiation in keratinocytes, by lens epithelium-derived growth factor (LEDGF). J. Mol. Biol. 320: 1053–1063
27. Kerr LD, Miller DB and Matrisian LM (1990) TGF β1 inhibition of transin/stromelysin gene expression is mediated through a Fos binding sequence. Cell 61: 267–278
28. White LA, Mitchell TI and Brinckerhoff CE (2000) Transforming growth factor β inhibitory element in the rabbit matrix metalloproteinase-1 (collagenase-1) gene functions as a repressor of constitutive transcription. Biochim. Biophys. Acta 1490: 259–268
29. Sharma P, Fatma N, Kubo E, Shinohara T, Chylack Jr. LT and Singh DP (2003) Lens epithelium-derived growth factor relieves transforming growth factorβ1-induced transcription repression of heat shock proteins in human lens epithelial cells. J. Biol. Chem. 278: 20037–20046
30. Barcellos-Hoff MH and Dix TA (1996) Redox-mediated activation of latent transforming growth factor-β1. Mol. Endocrinol. 10: 1077–1083
31. Annes JP, Munger JS and Rifkin DB (2003) Making sense of latent TGF β activation. J. Cell Sci. 116: 217–224
32. Chong H, Vodovotz Y, Cox GW and Barcellos-Hoff MH (1999) Immunocytochemical detection of latent TGF β-activation in cultured macrophages. J. Cell. Physiol. 178: 275–283
33. Barcellos-Hoff MH (1996) Latency and activation in the control of TGFβ. J. Mamm. Gland Biol. Neoplasia 1: 353–363
34. Ramachandran S, Morris SM, Devamanoharan P, Henein M and Verma SD (1991) Radio-isotopic determination of hydrogen peroxide in aqueous humor and urine. Exp. Eye Res. 53: 503–506
35. Ohba M, Shibanum M, Kuroki and Nose K (1994) Production of hydrogen peroxide by transforming growth factor β1 and its involvement in induction of egr-1 in mouse osteoblastic cells. J. Cell Biol. 126: 1079–1088
36. Lafon C, Mathieu C, Guerrin M, Pierre O, Vidal S and Valette A (1996) Transforming growth factor beta 1-induced apoptosis in human ovarian carcinoma cells: protection by the antioxidant *N*-acetylcysteine and bcl-2. Cell Growth Differ. 7: 1095–1104
37. Herrera B, Murillo MM, Alvarez-Barrientos A, Beltra J, Fernandez M and Fabregat I (2004) Source of early reactive oxygen species in the apoptosis induced by transforming growth factor β in fetal rat hepatocytes. Free Radic. Biol. Med. 36: 16–26
38. Herrera B, Alvarez AM, Sanchez A, Fernandez M Roncero C, Benito M and Fabregat I (2001) Reactive oxygen species mediates the mitochondrial-dependent apoptosis induced by transforming growth factor β in fetal hepatocytes. FASEB J. 15: 741–751
39. Kang SW, Chae HS, Seo MS, Kim KH, Baines IC and Rhee SG (1998b) Mammalian peroxiredoxin isoforms can reduce hydrogen peroxide generated in response to growth factors and tumor necrosis factor α. J. Biol. Chem. 273: 6297–6302
40. Wong CM, Chun AC, Kok KH, Zhou Y, Fung PC, Kung HF and Jeang KT (2000) Characterization of human and mouse peroxiredoxin IV: evidence for inhibition by Prx-IV of epidermal growth factor- and p53-induced reactive oxygen species. Antioxid. Redox Signal. 2: 507–518
41. Barcellos-Hoff MH (1996) Latency and activation in the control of TGF β. J. Mamm. Gland Biol. Neoplasia 1: 353–363
42. Hildeman DA, Mitchell T, Teague TK and Hensen P *et al* (1999) Reactive oxygen species regulate activation-induced T cell apoptosis. Immunity 10: 735–744
43. Wang X, Phelan SA, Forsman-Semb K, Taylor EF, Petros C, Brown A, Lerner CP and Paigen B (2003) Mice with targeted mutation of peroxiredoxin 6 develop normally but are susceptible to oxidative stress. J. Biol. Chem. 278: 25179–25190
44. Hales AM, Chamberlain CG, Dreher B and McAvoy JW (1999) Intravitreal injection of TGF beta induces cataract in rats. Invest. Ophthalmol. Vis. Sci. 40: 3231–3236
45. Hales AM, Chamberlain CG and McAvoy JW (1995) Cataract induction in lenses cultured with transforming growth factor β. Invest. Ophthalmol. Vis. Sci. 36: 1709–1713
46. Srinivasan Y, Lovicu FJ and Overbeek PA (1998) Lens-specific expression of transforming growth factor β1 in transgenic mine causes anterior subcapsular cataracts. J. Clin. Invest. 101: 625–634
47. Zhao J, Bu D, Lee M, Slavkin HC, Hall FL and Warburton D (1996) Abrogation of transforming growth factor-β type II receptor stimulates embryonic mouse lung branching morphogenesis in culture. Dev. Biol. 180: 242–257
48. Herrera B, Alvarez AM, Sanchez A, Fernandez M, Roncero C, Benito M and Fabregat I (2001) Reactive oxygen species (ROS) mediates the mitochondrial-dependent apoptosis induced by transforming growth factor β in fetal hepatocytes. FASEB J. 15: 741–751
49. Herrera B, Murillo MM, Alvarez-Barrientos A, Beltra J, Fernandez M and Fabregat I (2004) Source of early reactive oxygen species in the apoptosis induced by transforming growth factor β in fetal rat hepatocytes. Free Radic. Biol. Med. 36: 16–26
50. Tan S, Sagara Y, Liu Y, Maher P and Schubert D (1998) The regulation of reactive oxygen species production during programmed cell death. J. Biol. Chem. 141: 1423–1432
51. Khalil N (1999) TGFβ: from latent to active. Microbes. Infect. 1: 1255–1263
52. Chen W, Frank ME, Jin W and Wahl SM (2001) TGF-β released by apoptotic T cells contributes to an immunosuppressive milieu. Immunity 14: 715–725
53. Frederick JP, Liberati NT, Waddell DS, Shi Y and Wang XF (2004) Transforming growth factor β-mediated transcriptional repression of *c-myc* is dependent on direct binding of Smad3 to a novel repressive Smad binding element. Mol. Cell. Biol. 24: 2546–2559

54. Yagi K, Furuhashi M, Aoki H, Goto D, Kuwano H, Sugamura K, Miyazono K and Kato M (2002) c-myc is a downstream target of the Smad pathway. J. Biol. Chem. 277: 854–861
55. Kirkman HN and Gaetani GF (1984) Catalase: a tetrameric enzyme with four tightly bound molecules of NADPH. Proc. Natl. Acad. Sci. USA 81: 4343–4347
56. Tabatabai T and Floyd RA (1994) Susceptibility of glutathione peroxidase and glutathione reductase to oxidative damage and the protective effect of spin trapping agents. Arch. Biochem. Biophys. 314: 112–119
57. Day BJ, Shawen S, Liochev SI and Crapo JD (1995) A metal-loporphyrin superoxide dismutase mimetic protects against paraquat-induced endothelial cell injury, *in vitro*. J. Pharmacol. Exp. Ther. 275: 1227–1232
58. Patel M (1998) Inhibition of neuronal apoptosis by a metalloporphyrin superoxide dismutase mimic. J. Neurochem. 71: 1068–1074
59. Kurosaka D and Nagamoto T (1994) Inhibitory effect of TGF-β2 in human aqueous humor on bovine lens epithelial cell proliferation. Invest. Ophthalmol. Vis. Sci. 35: 3408–3412
60. Cousins SW, McCabe MM, Danielpour D and Streilein JW (1991) Identification of transforming growth factor-beta as an immunosuppressive factor in aqueous humor. Invest. Ophthalmol. Vis. Sci. 32: 2201–2211
61. Spector A and Garner H (1981) Hydrogen peroxide and human cataract. Exp. Eye Res. 33: 673–681
62. Spector A (1995) Oxidative stress-induced cataract: mechanism of action. FASEB J. 9: 1173–1182
63. Skonier J, Bennett K, Rothwell V, Kosowski S, Plowman G, Wallace P, Edelhoff S, Disteche C, Neubauer M, Marquardt H, Rodgers J and Purchio AF (1994) βig-h3:a transforming growth factor-beta-responsive gene encoding a secreted protein that inhibits cell attachment *in vitro* and suppresses the growth of CHO cells in nude mice. DNACellBiol. 13: 571–584
64. Billings PC, Herrick D, Kucich U, Englelsberg, BN, Abrahams, WR, Macarak, EJ, Rosenbloom J and Howard PS (2000) Extracellular matrix and nuclear localization of βig-h3 in human bladder smooth muscle and fibroblast cells. J. Cell. Biochem. 79: 261–273
65. Lee EH, Seomun Y, Hwang KH, Kim JE, Kim IS, Kim JH and Joo CK (2000) Over-expression of the transforming growth factor-beta-inducible gene betaig-h3 in anterior polar cataracts. Invest. Ophthalmol. Vis. Sci. 41: 1840–1850
66. Wu X, Daniels T, Molinaro C, Lilly MB and Casiano CA (2002) Caspase cleavage of the nuclear autoantigen LEDGF/p75 abrogates its pro-survival function: implications for autoimmunity in atopic disorders. Cell Death Differ. 9: 915–925
67. Singh DP, Ohguru N, Chylack Jr. LT and Shinohara T (1999) Lens epithelium-derived growth factor: increased resistance to thermal and oxidative stresses. Invest. Ophthalmol. Vis. Sci. 40: 1–8
68. Singh DP, Ohguru N, Kikuchi T, Sueno T, Reddy VN, Yuge K, Chylack Jr. LT and Shinohara T (2000) Lens epithelium-derived growth factor: effects on growth and survival of lens epithelial cells, keratinocytes and fibroblast. Biochem. Biophys. Res. Commun. 267: 373–381
69. Matsui H, Lin LR, Singh DP, Shinohara T and Reddy VN (2001) Lens epithelium-derived growth factor: increased survival and decreased DNA breakage of human RPE cells induced by oxidative stress. Invest. Ophthal. Vis. Sci. 42: 2935–2941
70. Ahuja P, Caffe AR, Holmqvist I, Soderpalm AK, Singh DP, Shinohara T and Van Veen T (2001) Lens epithelium-derived growth factor (LEDGF) delays photoreceptor degeneration in explants of rd/rd mouse retina. NeuroReport 12: 2951–2955
71. Machida S, Chaudhry P, Shinohara T, Singh DP, Reddy VK, Chylack Jr. LT, Sieving PA and Bush RA (2001) Lens epithelium-derived growth factor (LEDGF) promotes photoreceptor survival in light-damaged and Royal College of Surgeons (RCS) rats. Invest. Ophthalmol. Vis. Sci. 42: 1087–1095
72. Abate CL, Patel L, Rauscher FJ and Curran T (1990) Redox regulation of fos and jun DNA binding activity *in vitro*. Science 249: 1157–1161
73. Schreck R, Rieber P and Baueerle PA (1991) Reactive oxygen intermediates as apparently widely used messenger in the activation of NF-kB transcription factor and HIV-1. EMBO J. 10: 2247–2258
74. Iakoubova OA, Pacella LA, Her H and Beier DR (1997) LTW4 protein on mouse chromosome 1 is a member of a family of antioxidant proteins. Genomics 42: 474–478
75. Phelan SA, Johnson KA, Beier DR and Paigen B (1998) Characterization of the murine gene encoding Aop2 (antioxidant protein 2) and identification of two highly related genes. Genomics 54: 132–139
76. Spector A, Kuszak JR, Ma W, Wang RR, Ho Y and Yang Y (1998) The effect of photochemical stress upon the lenses of normal and glutathione peroxidase-1 knockoutmice. Exp. Eye Res. 67: 57–71
77. Nakamura M, Singh DP, Kubo E, Chylack Jr. LT and Shinohara T (2000) LEDGF: survival of embryonic chick retinal photoreceptor cells. Invest. Ophthal. Vis. Sci. 41: 1–8
78. Cory AH, Owen TC, Barltrop JA and Cory JG (1991) Use of an aqueous soluble tetrazolium/formazan assay for cell growth assays in culture. Cancer Commun. 3: 207–212
79. Kubo E, Urakami T, Fatma N, Akagi Y and Singh DP (2004) Polyol pathway-dependent osmotic and oxidative stresses in aldose reductase-mediated apoptosis in human lens epithelial cells: role of AOP2. Biochem. Biophys. Res. Commun. 314: 1050–1056
80. Yun SJ, Kim MO, Kim SO, Park J, Kwon YK, Kim IS and Lee EH (2002) Induction of TGF-β-inducible gene-h3 (betaig-h3) by TGF-β1 in astrocytes: implications for astrocyte response to brain injury. Brain Res. Mol Brain Res. 107: 57–64
81. Fatma N, Kubo E, Chylack Jr. LT, Shinohara T, Akagi Y and Singh DP (2004) LEDGF regulation of alcohol and aldehyde dehydrogenases in lens epithelial cells: stimulation of retinoic acid production and protection from ethanol toxicity. Am. J. Physiol. Cell Physiol. 287: 508–516
82. Bradford MM (1976) A rapid sensitive method for the quantitation of microgram quantities of protein utilizing the principle of protein dye binding. Anal. Biochem. 72: 248–254